Fig. 4

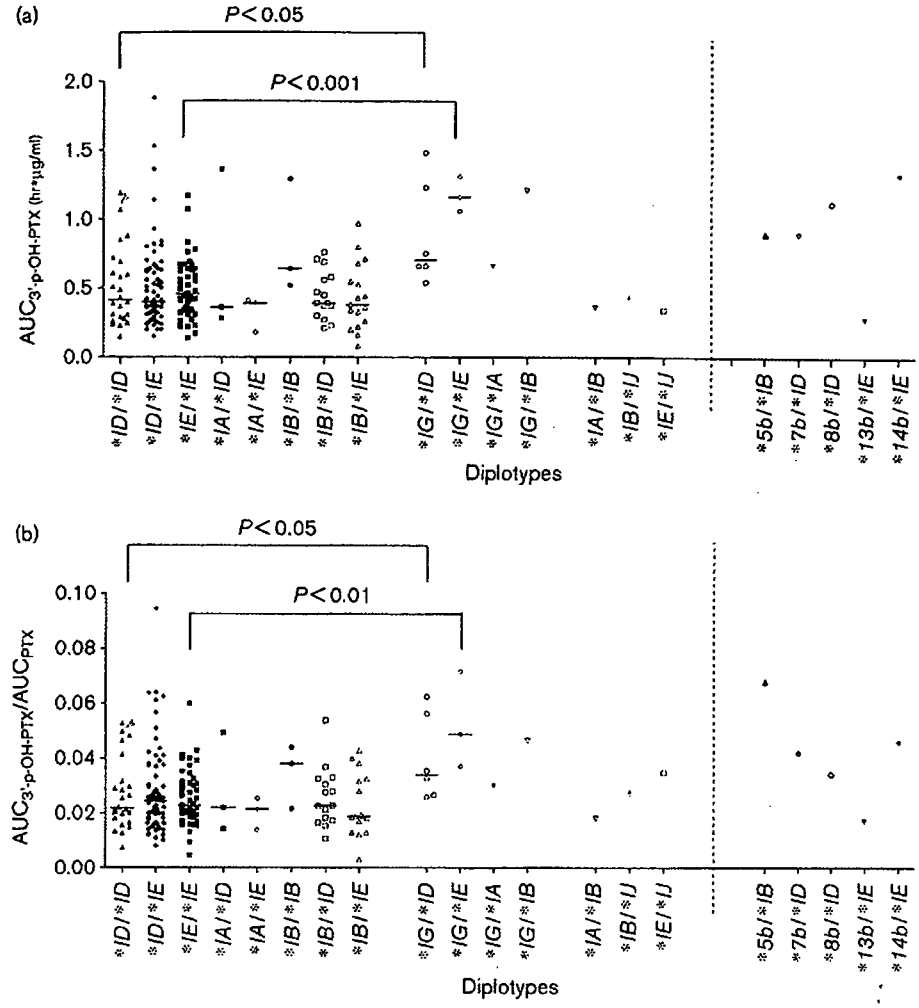

Effects of *CYP2C8* diplotypes on AUC of 3′-*p*-OH-PTX (a), and AUC ratio of 3′-*p*-OH-PTX/PTX (b). All combinations of diplotypes using grouped haplotypes for **1* are shown. Grey arrowheads indicate patients with heterozygous **1t* haplotype. Statistical significance was analyzed by the Mann–Whitney *U*-test to reveal the effects of **IG* group haplotypes. AUC, area under concentration–time curve; PTX, paclitaxel.

and IVS4 + 151G > A were relatively **IG* group specific. Because the patient with **1t* haplotype also had a high AUC of 3′-*p*-OH-PTX and a high AUC ratio of 3′-*p*-OH-PTX/PTX, it is possible that the IVS3 – 21T > A could be a functionally causing variation rather than IVS4 + 151G > A. Because IVS3-21T > A is located in the T-rich (pyrimidine-rich) region upstream of a splice acceptor site and this polypyrimidine tract is important for efficient RNA spliceosome assembly [21], this transversion could reduce the expression level of mature CYP2C8 mRNA, resulting in reduced protein expression levels. We cannot, however, exclude the possibility that other identified/unidentified linked variation could be causative.

We did not observe significant differences in the AUC of 6α-OH-PTX and AUC ratio of 6α-OH-PTX/PTX between the heterozygous **IG* patients and *non-*IG/non-*IG* patients. This is surprising because CYP2C8 is considered to be the major enzyme responsible for 6α-hydroxylation of PTX. Currently, we have no data for explaining this. It is noteworthy that the *CYP3A4*16B* haplotype more clearly affects the increase in AUC ratio of 6α-OH-PTX/PTX than the decrease in AUC ratio of 3′-*p*-OH-PTX/PTX [9]. CYP3A4- and CYP2C8-mediated disappearance processes of 6α-OH-PTX and 3′-*p*-OH-PTX, respectively, might be more influential to their AUCs than their generation from PTX. One alternative (less likely) possibility is that another unidentified enzyme also catalyzes the transformation of PTX into 6α-OH-PTX *in vivo*, and that the effect of reduced CYP2C8 activity is not clearly reflected in the parameters analyzed.

Neither the normalized clearance nor AUC of PTX was significantly influenced by *CYP2C8* diplotypes. The small effect of **IG* on PTX clearance may be partly explained

Fig. 5

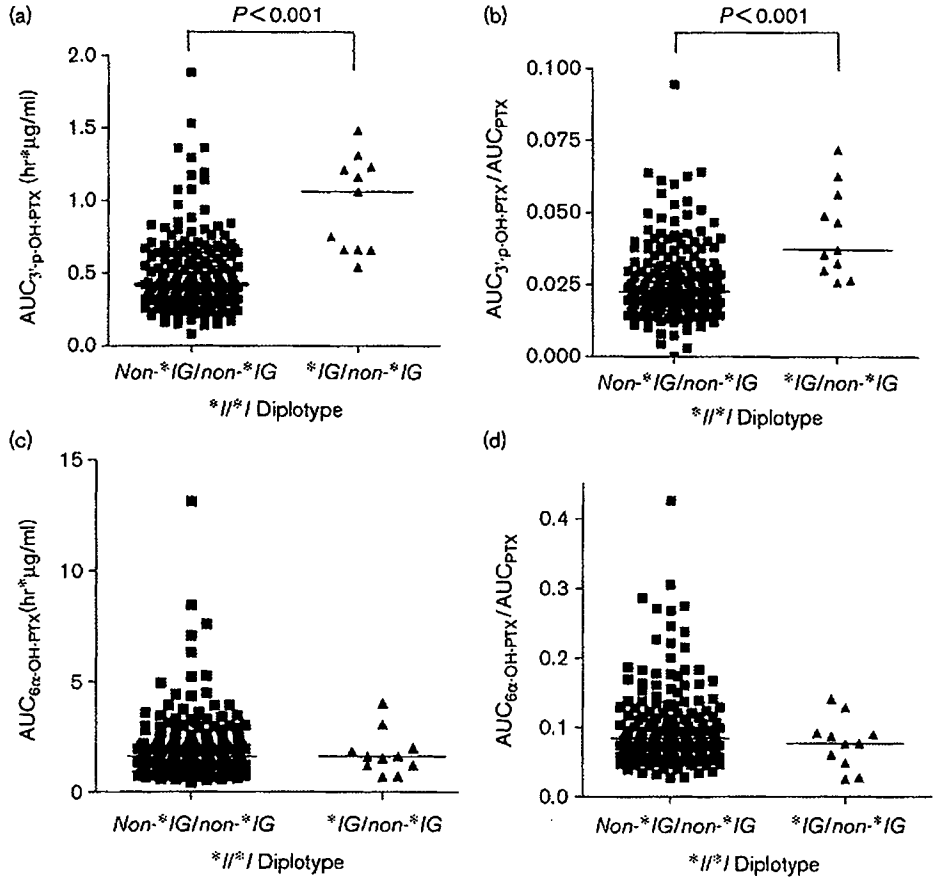

Effects of *CYP2C8*IG* group haplotypes on AUC of 3′-*p*-OH-PTX (a), AUC ratio of 3′-*p*-OH-PTX/PTX (b), AUC of 6α-OH-PTX (c), and AUC ratio of 6α-OH-PTX/PTX (d). Statistical significance was analyzed by the Mann–Whitney *U*-test. AUC, area under concentration–time curve; PTX, paclitaxel.

by only small fraction of PTX to be metabolized. In fact, median AUC of 3′-*p*-OH-PTX (0.50 h/mol/l) and 6α-OH-PTX (1.85 h/mol/l) was only 2.3 and 8.5% of that of AUC of PTX (21.67 h/mol/l), respectively.

Recently, Nakajima *et al.* [13] tried to analyze the effects of *CYP2C8* polymorphisms on PTX pharmacokinetics. They genotyped 11 nonsynonymous variations including *CYP2C8*5*, but none were detected from 23 Japanese ovarian cancer patients. Also, we could not apply statistical analysis to the pharmacokinetic parameters for five nonsynonymous variations as described above since the nonsynonymous variations are all rare in Japanese. Rather, **IG* group haplotypes (and possibly **1*) are probably important for PTX metabolism. The effect of this group haplotypes tagged by IVS3−21T > A on pharmacokinetics of other CYP2C8-catalyzing drugs must be clarified in the future.

In conclusion, we determined/inferred a total of 49 haplotypes using the detected variations in the *CYP2C8* gene from 437 Japanese patients. *CYP2C8*IG* group haplotypes, consisting of intronic variations, were found to be associated with significantly increased AUC of the PTX metabolite 3′-*p*-OH-PTX and the AUC ratio of 3′-*p*-OH-PTX/PTX. Thus, *CYP2C8*IG* group haplotypes may influence CYP2C8 activity, although the causative variation is not fully identified.

Acknowledgements

We thank Ms Chie Sudo for her secretarial assistance, and Ms F. Kato for sample analysis. We are grateful to Ms E. Toshiro, Ms T. Chujo, and Ms M. Shimada for their assistance throughout patient recruitment. None of the authors have any conflict of interest. This work was supported in part by the Program for Promotion of Fundamental Studies in Health Sciences and by a Health and Labour Sciences Research Grant from the Ministry of Health, Labour and Welfare of Japan.

References

1 Totah RA, Rettie AE. Cytochrome P450 2C8: substrates, inhibitors, pharmacogenetics, and clinical relevance. *Clin Pharmacol Ther* 2005; 77:341–352.

2 Sonnichsen DS, Liu Q, Schuetz EG, Schuetz JD, Pappo A, Relling MV. Variability in human cytochrome P450 paclitaxel metabolism. *J Pharmacol Exp Ther* 1995; 275:566–575.
3 Baldwin SJ, Clarke SE, Chenery RJ. Characterization of the cytochrome P450 enzymes involved in the in vitro metabolism of rosiglitazone. *Br J Clin Pharmacol* 1999; 48:424–432.
4 Dai D, Zeldin DC, Blaisdell JA, Chanas B, Coulter SJ, Ghanayem BI, *et al.* Polymorphisms in human CYP2C8 decrease metabolism of the anticancer drug paclitaxel and arachidonic acid. *Pharmacogenetics* 2001; 11:597–607.
5 Soyama A, Saito Y, Hanioka N, Murayama N, Nakajima O, Katori N, *et al.* Non-synonymous single nucleotide alterations found in the CYP2C8 gene result in reduced in vitro paclitaxel metabolism. *Biol Pharm Bull* 2001; 24:1427–1430.
6 Bahadur N, Leathart JB, Mutch E, Steimel-Crespi D, Dunn SA, Gilissen R, *et al.* CYP2C8 polymorphisms in Caucasians and their relationship with paclitaxel 6alpha-hydroxylase activity in human liver microsomes. *Biochem Pharmacol* 2002; 64:1579–1589.
7 Soyama A, Saito Y, Komamura K, Ueno K, Kamakura S, Ozawa S, *et al.* Five novel single nucleotide polymorphisms in the CYP2C8 gene, one of which induces a frame-shift. *Drug Metab Pharmacokinet* 2002; 17:374–377.
8 Hichiya H, Tanaka-Kagawa T, Soyama A, Jinno H, Koyano S, Katori N, *et al.* Functional characterization of five novel CYP2C8 variants, G171S, R186X, R186G, K247R, and K383N, found in a Japanese population. *Drug Metab Dispos* 2005; 33:630–636.
9 Nakajima Y, Yoshitani T, Fukushima-Uesaka H, Saito Y, Kaniwa N, Kurose K, *et al.* Impact of the haplotype CYP3A4*16B harboring the Thr185Ser substitution on paclitaxel metabolism in Japanese cancer patients. *Clin Pharmacol Ther* 2006; 80:179–191.
10 Martinez C, Garcia-Martin E, Blanco G, Gamito FJ, Ladero JM, Agundez JA. The effect of the cytochrome P450 CYP2C8 polymorphism on the disposition of (R)-ibuprofen enantiomer in healthy subjects. *Br J Clin Pharmacol* 2005; 59:62–68.
11 Niemi M, Leathart JB, Neuvonen M, Backman JT, Daly AK, Neuvonen PJ. Polymorphism in CYP2C8 is associated with reduced plasma concentrations of repaglinide. *Clin Pharmacol Ther* 2003; 74:380–387.
12 Henningsson A, Marsh S, Loos WJ, Karlsson MO, Garsa A, Mross K, *et al.* Association of CYP2C8, CYP3A4, CYP3A5, and ABCB1 polymorphisms with the pharmacokinetics of paclitaxel. *Clin Cancer Res* 2005; 11: 8097–8104.
13 Nakajima M, Fujiki Y, Noda K, Ohtsuka H, Ohkuni H, Kyo S, *et al.* Pharmacokinetics of paclitaxel in ovarian cancer patients and genetic polymorphisms of CYP2C8, CYP3A4, and MDR1. *J Clin Pharmacol* 2005; 45:674–682.
14 Judson R, Stephens JC, Windemuth A. The predictive power of haplotypes in clinical response. *Pharmacogenomics* 2000; 1:15–26.
15 Monsarrat B, Chatelut E, Royer I, Alvinerie P, Dubois J, Dezeuse A, *et al.* Modification of paclitaxel metabolism in a cancer patient by induction of cytochrome P450 3A4. *Drug Metab Dispos* 1998; 26:229–233.
16 Taniguchi R, Kumai T, Matsumoto N, Watanabe M, Kamio K, Suzuki S, *et al.* Utilization of human liver microsomes to explain individual differences in paclitaxel metabolism by CYP2C8 and CYP3A4. *J Pharmacol Sci* 2005; 97:83–90.
17 Ferguson SS, Chen Y, LeCluyse EL, Negishi M, Goldstein JA. Human CYP2C8 is transcriptionally regulated by the nuclear receptors constitutive androstane receptor, pregnanex receptor, glucocorticoid receptor, and hepatic nuclear factor 4α. *Mol Pharmacol* 2005; 68:747–757.
18 Kitamura Y, Moriguchi M, Kaneko H, Morisaki H, Morisaki T, Toyama K, *et al.* Determination of probability distribution of diplotype configuration (diplotype distribution) for each subject from genotypic data using the EM algorithm. *Ann Hum Genet* 2002; 66:183–193.
19 Bandelt HJ, Forster P, Rohl A. Median-joining networks for inferring intraspecific phylogenies. *Mol Biol Evol* 1999; 16:37–48.
20 Lehnert M, Emerson S, Dalton WS, de Giuli R, Salmon SE. *In vitro* evaluation of chemosensitizers for clinical reversal of P-glycoprotein-associated Taxol resistance. *J Natl Cancer Inst Monogr* 1993; 15:63–67.
21 Roscigno RF, Weiner M, Garcia-Blanco MA. A mutational analysis of the polypyrimidine tract of introns. Effects of sequence differences in pyrimidine tracts on splicing. *J Biol Chem* 1993; 268:11222–11229.

Lung Cancer (2007) 57, 328–333

available at www.sciencedirect.com

ScienceDirect

journal homepage: www.elsevier.com/locate/lungcan

Detection of unsuspected distant metastases and/or regional nodes by FDG-PET in LD-SCLC scan in apparent limited-disease small-cell lung cancer

Seiji Niho[a,*], Hirofumi Fujii[b], Koji Murakami[b,c], Seisuke Nagase[a], Kiyotaka Yoh[a], Koichi Goto[a], Hironobu Ohmatsu[a], Kaoru Kubota[a], Ryuzo Sekiguchi[d], Shigeru Nawano[d], Nagahiro Saijo[a], Yutaka Nishiwaki[a]

[a] *Division of Thoracic Oncology, National Cancer Center Hospital East, Kashiwanoha 6-5-1, Kashiwa, Chiba 277-8577, Japan*
[b] *Functional Imaging Division, National Cancer Center Research Center for Innovative Oncology, Chiba, Japan*
[c] *PET Center, Dokkyo Medical University, Tochigi, Japan*
[d] *Department of Radiology, National Cancer Center Hospital East, Chiba, Japan*

Received 12 January 2007; received in revised form 30 March 2007; accepted 6 April 2007

KEYWORDS
Small-cell lung cancer;
Limited-disease;
FDG-PET;
CT;
Staging;
Occult distant metastasis

Summary We retrospectively investigated the clinical usefulness of fluorodeoxyglucose positron emission tomography (FDG-PET) for evaluation of patients with limited-disease small-cell lung cancer (LD-SCLC) diagnosed by conventional staging procedures. Sixty-three patients received whole body FDG-PET scans after routine initial staging procedures. The findings of FDG-PET scans suggesting extensive-stage disease were confirmed by other imaging tests or by the patient's clinical course. FDG-PET scan findings indicated distant metastases in 6 of 63 patients. Metastatic disease was confirmed in five of these six patients (8%, 95% confidence interval: 3–18%). FDG-PET scan also detected regional lymph node metastases even in nine patients (14%) in whom computed tomography images had been negative, including contralateral lymph node metastasis in three patients. FDG-PET scan detected additional lesions in patients diagnosed as having LD-SCLC by conventional staging procedures. The therapeutic strategies were changed in 8% of patients based on the results of FDG-PET. FDG-PET scan is recommended as an initial staging tool for patients with this disease.

1. Introduction

Small-cell lung cancer (SCLC) accounts for 15–20% of all lung cancers. SCLC shows more aggressive biological behaviour than non-small cell lung cancer (NSCLC). A clinical two-stage system proposed by the Veterans Administration Lung

* Corresponding author. Tel.: +81 4 7133 1111; fax: +81 4 7131 4724.
E-mail address: siniho@east.ncc.go.jp (S. Niho).

0169-5002/$ – see front matter © 2007 Elsevier Ireland Ltd. All rights reserved.
doi:10.1016/j.lungcan.2007.04.001

Study Group (VALSG) distinguishes limited-disease (LD) and extensive-disease (ED) in SCLC [1]. LD is defined as limited to one hemithorax, including mediastinal, contralateral hilar and ipsilateral supraclavicular lymph nodes, while ED represents tumour spread beyond these regions. Approximately two-thirds of patients with SCLC are diagnosed as having ED at the initial staging. The current standard care for LD-SCLC is a combination of chemotherapy and chest irradiation. With current treatment, patients with LD have a median survival of 23–27 months [2,3], compared to 10–12 months for those with ED [4]. Therefore, accurate pretreatment staging is important for patients with SCLC in order to determine the appropriate therapy.

Conventional staging procedures for lung cancer consist of computed tomography (CT) of the chest and upper abdomen, bone scan, and CT scan or magnetic resonance imaging (MRI) of the brain. Recently, fluorodeoxyglucose positron emission tomography (FDG-PET) was introduced as a staging tool for NSCLC. According to the guidelines of the American Society of Clinical Oncology, PET scan is recommended for survey occult locoregional lesions and distant metastases in patients with NSCLC [5]. Two separate prospective studies demonstrated that FDG-PET detected unsuspected distant metastases in 24% of patients with apparent stage III NSCLC [6,7]. Another study showed that FDG-PET changed or influenced management decisions in 67% of patients with NSCLC. PET plays an important role in staging of NSCLC [8]. However, previous PET studies of SCLC involved only a relatively small number of patients [9–17]. In a prospective study, FDG-PET was performed for 24 patients diagnosed as having LD-SCLC by conventional staging procedures [9]. Based on FDG-PET findings, two of these 24 patients were upstaged to ED. Bone metastases were found in one patient, and contralateral supraclavicular lymph node metastasis in another. Larger studies are required to confirm the role of FDG-PET in the staging of LD-SCLC. In this study, we retrospectively investigated the usefulness of FDG-PET to detect distant metastases or unsuspected regional nodal metastases in patients with LD-SCLC diagnosed by conventional staging procedures.

2. Patients and methods

2.1. Patients

Seventy patients were newly diagnosed as having LD-SCLC by conventional staging procedures at the National Cancer Center Hospital East between July 2003 and December 2006. Conventional staging procedures included history and physical examination, chest radiography, CT scan of the chest, CT scan or ultrasound (US) of the abdomen, bone scan, and CT scan or MRI of the brain. CT scan and MR images were enhanced with contrast media. LD is defined in this study as disease limited to one hemithorax, including mediastinal, contralateral hilar and supraclavicular lymph nodes, ipsilateral pleural effusion, and pericardial effusion, while ED represents tumour spread beyond these manifestations [18]. This study included 63 patients who received whole body FDG-PET scan after the routine initial staging procedures. Fifty-seven were male and the remaining 6 were female. Median age was 64 years, range 48–80 years. Forty-two patients received FDG-PET before commencement of chemotherapy. The remaining 21 patients received FDG-PET 1 to 11 days (median: 4 days) after commencement of chemotherapy. Forty-four and 19 patients received CT scan and US of the abdomen, respectively.

2.2. FDG-PET scan

FDG-PET scans were performed before March 2005 (patients No. 1–25), and FDG-PET/CT scans were performed after April 2005 (patients No. 26–63). Three hundred MBq of F-18 FDG were intravenously injected after at least 6 h of fasting. Acquisition was initiated 60 min after the injection. FDG-PET imaging was performed using a GE Advance Scanner (General Electric Medical System, Milwaukee, WI), whose axial field of view was 15.2 cm and spatial resolution 4.9 mm of full-width-half-maximum. Scans were performed using two-dimensional acquisition mode from the thigh to the skull base with seven bed positions. Each bed position was composed of 1 min of transmission scanning and 5 min of emission scanning.

FDG-PET/CT imaging was performed using a GE Discovery LS Scanner (General Electric Medical System, Milwaukee, WI) or a GE Discovery ST Scanner (the same manufacturer). The PET component of the GE Discovery LS Scanner was the same as that of the GE Advance Scanner. For the PET component of the GE Discovery ST Scanner, the axial field of view was 15.7 cm and the spatial resolution was 6.2 mm of full-width-half-maximum. PET scans were performed with both scanners using 2-dimensional acquisition mode from the thigh to the skull base with 7 bed positions. Each bed position was composed of 4 min of emission scanning. The CT component of both PET/CT scanners was a 16-row multidetector CT scanner and CT images were acquired with a tube voltage of 140 kV, and the tube current was automatically set using the auto-exposure control function so that the number of standard deviations of noise was limited to 10. Attenuation correction of PET images was performed using the data from CT images.

Image reconstruction was performed using an ordered subsets expectation maximization (OSEM) algorithm with subset and iteration values of 14 and 2, respectively.

2.3. Image interpretation

All PET and CT images were interpreted by experienced radiologists and physicians. The 4.25 mm-thick images of axial, coronal and sagittal planes on hard copy films were reviewed. Uptake stronger than mediastinal blood pool activity was diagnosed as malignancy by the visual estimation. Symmetrical activities observed in both hilar regions were considered to be benign reactive changes. Any discrepancies between the radiologist and physician were resolved by discussion. The findings detected by FDG-PET were confirmed by other image tests or observation of the clinical course. FDG-PET was conducted after conventional staging procedures. CT, US and bone scans were interpreted without the FDG-PET findings. However, FDG-PET scan was interpreted in comparison with CT findings, while PET/CT findings were interpreted independently.

Table 1 Discrepancy between FDG-PET and conventional staging procedures (distant metastases)

Patient no.	Age (years)	Gender	CT N	PET N	PET M	Interval between conventional staging procedures and FDG-PET (days)	Comments
2	61	Male	2	2	1	20	Multiple bone metastases (PET)
6	68	Male	2	2	1	7	Lymph* node metastasis around the cardia (PET)
47	61	Male	3	3	1	28	Multiple bone metastases (PET)
55	68	Male	2	2	1	20 (CT) and 14 (bone scan)	Liver, axillary lymph node, and iliac bone metastases (PET)
59	52	Male	3	3	1	13	Adrenal, cervical and mandibular lymph node metastases (PET)
63	59	Male	3	3	1	18 (CT) and 11 (bone scan)	Multiple bone and liver metastases (PET)

FDG, fluorodeoxyglucose; PET, positron emission tomography; CT, computed tomography; N, node; M, metastasis.
* Diagnosis of lymph node metastasis was not confirmed by other imaging modalities or observation of the clinical course.

3. Results

3.1. Detection of distant metastasis

FDG-PET showed results different from those of conventional staging procedures in 17 of 63 patients. PET scan demonstrated findings suggesting distant metastases in 6 of 63 patients (Table 1). The median interval between conventional staging procedures and FDG-PET was 16 days (range: 7–28). Abnormal uptake was observed around the cardia in one of these six patients (No.6). A repeat FDG-PET study demonstrated a longer uptake stripe indicating radiation-induced oesophagitis and the diagnosis could not be established, as there was a remaining possibility of physiological uptake in the oesophagus. The diagnosis of metastatic disease was confirmed in the remaining five patients (8%, 95% confidence interval (CI): 3–18%). Among these five patients, four had bone metastases, two had liver metastases, one had adrenal metastasis, and two had lymph node metastases in the cervical or axillary region. The therapeutic strategy for these five patients was changed and they received only chemotherapy without thoracic radiotherapy. One patient (No. 47) had shown negative findings on bone scintigraphy four weeks before the FDG-PET study, but PET scan demonstrated increased FDG uptake in bones throughout the body. MRI of the spine confirmed the diagnosis of multiple bone metastases (Fig. 1). A repeat bone scan after three months detected obvious multiple bone metastases in No. 2 patient. Two hepatic lesions, as well as the primary tumour, mediastinal and hilar lymph nodes, had all increased in size after two cycles of chemotherapy in patient No. 55. A hepatic lesion, as well as the primary tumour, had decreased in size after two cycles of chemotherapy in patient No. 63. These hepatic lesions were compatible with liver metastases. Abnormal uptake by the right adrenal gland disappeared on repeat PET/CT after four cycles of chemotherapy in patient No. 59. Abnormal uptake in primary and mediastinal lesions was extremely decreased in this patient. The right adrenal gland lesion was compatible with metastasis.

FDG-PET detected liver metastasis in one of 44 patients staged by CT scan of the abdomen (No. 55), and liver or adrenal metastasis in two of 19 patients staged by US (Nos. 59 and 63). Liver and adrenal metastases not detected by US were small, such that the CT part of PET/CT could not detect them as metastases. Ratios of upstaging by FDG-PET between initial CT scan and US of the abdomen were not statistically significant (1/44 versus 2/19, $P=0.214$).

3.2. Detection of regional lymph node metastases

FDG-PET scans detected regional lymph node metastases that had been negative on CT scans in nine patients (14%) (Table 2). The median interval between CT of the chest and FDG-PET was 19 days (range: 7–34). FDG-PET scans newly detected ipsilateral supraclavicular lymph node metastasis in four patients, contralateral lymph node metastasis in three, and mediastinal lymph node metastasis in two. These nine patients all underwent curative chemoradiotherapy, and abnormal FDG uptake in mediastinal and/or supraclavicular lymph nodes disappeared or decreased on repeat PET scans after chemoradiotherapy. These lymph nodes were considered positive for metastasis.

CT scan detected swollen mediastinal lymph nodes without abnormal FDG uptake in two patients. One patient had a past history of pulmonary tuberculosis complicated by pulmonary fibrosis. The swollen pretracheal lymph node was considered negative for metastasis because the node size remained unchanged after four cycles of chemotherapy although the primary tumour shrank. This case showed false positive findings on CT whereas FDG-PET correctly diagnosed the extent of disease (No. 43). The other patient had atelectasis of the right middle lobe due to the primary tumour. Superior mediastinal and subcarinal lymph nodes were considered to be metastatic on CT, but abnormal FDG uptake was absent. After three cycles of chemotherapy the

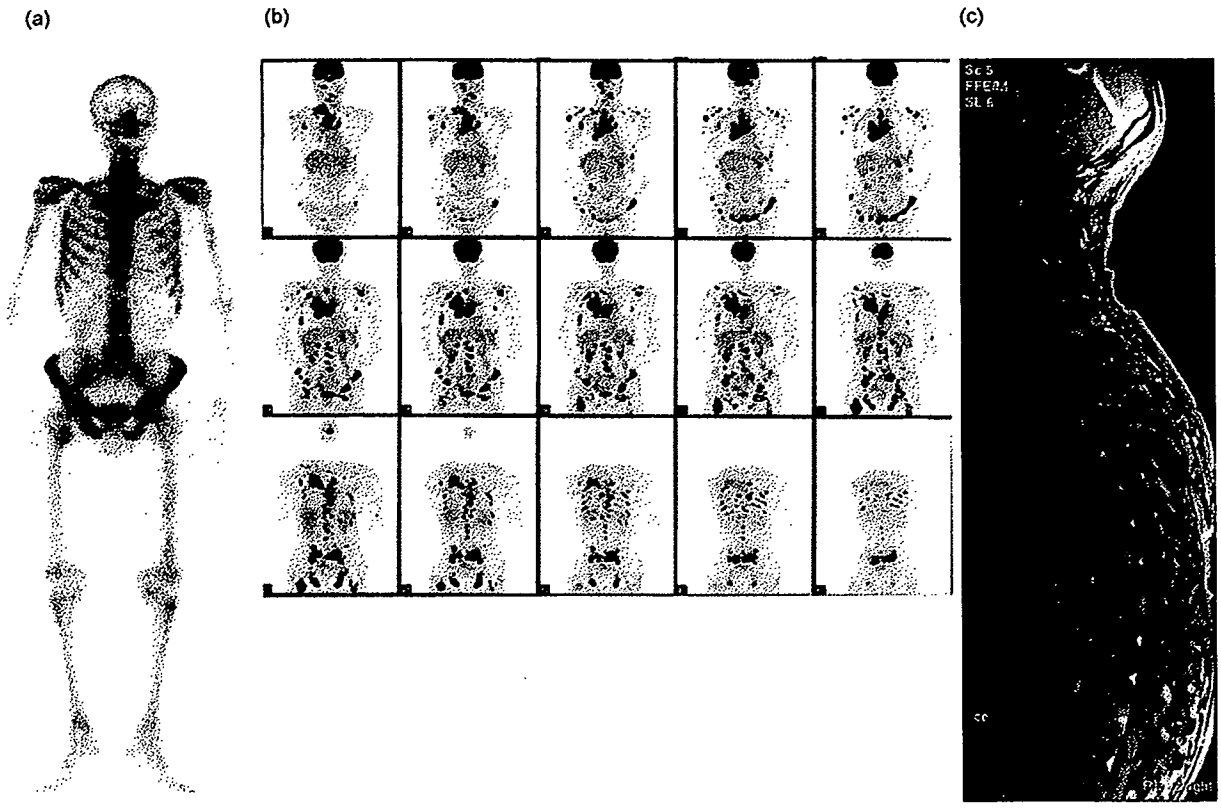

Fig. 1 A 61-year-old man with small-cell lung cancer. Bone scintigraphy was negative for osseous metastasis (a). However, PET scan demonstrated increased FDG uptake in bones throughout the body (b). MRI of the spine confirmed multiple bone metastases (c).

mediastinal lesion showed no change although the primary tumour had decreased in size and atelectasis of the right middle lobe was improved. The mediastinal lymph nodes were considered negative for metastasis (No. 61).

4. Discussion

SCLC tends to disseminate early in the disease course and displays a more aggressive clinical behaviour than NSCLC. Local treatment modalities alone such as radiotherapy or surgery are not effective in prolonging survival beyond a few weeks. Systemic chemotherapy is the mainstay of treatment for patients in all stages of SCLC. A combination of chemotherapy and thoracic irradiation can promote long-term survival for patients diagnosed as having limited disease and recent clinical trials of chemoradiotherapy for LD-SCLC obtained 5-year survival rates of 24–26% [2,3]. However, thoracic irradiation might cause severe radiation pneumonitis, resulting in respiratory failure and/or treatment-related death. Furthermore, thoracic irradiation might also cause oesophagitis which worsens patient quality of life. Accurate clinical staging is important to determine the indications for chemoradiotherapy in SCLC. Our study demonstrated that FDG-PET scan detected unsuspected distant metastases in 8% of patients with LD-SCLC based on conventional staging procedures and that the detection of these new lesions changed their therapeutic strategies. Furthermore, FDG-PET scan detected regional lymph node metastases which had not been visualized on CT scan in 14% of patients. The radiation field could be appropriately set to cover the positive nodes based on the PET study results. Our results reconfirmed those of a previous preliminary study with a smaller number of patients [9].

Is the rate of the detection of unsuspected distant metastases (8%) clinically significant? Previous studies demonstrated that FDG-PET scan detected unsuspected distant metastases in 24% of patients with stage III NSCLC [6,7]. Compared to this result, the impact of FDG-PET on the staging of SCLC seems to be weaker. SCLC tends to have more obvious distant metastases than NSCLC, because of the aggressive biological behaviour of SCLC. Therefore, FDG-PET might detect unsuspected distant metastases at a relatively low rate. The most common region for unsuspected PET-detected metastasis in NSCLC was the abdomen, with 53% of pateints having adrenal, liver, and other lesions [6]. In our study, FDG-PET detected bone metastases in four of five patients who were upstaged from LD to ED. These lesions might reflect metastasis to the bone marrow, although no pathological evidence was obtained, because neither bone marrow biopsy nor aspiration cytology was routinely conducted for the initial clinical staging.

Our retrospective analyses have several limitations. We did not confirm histologically regional lymph node or distant metastases detected by FDG-PET or CT. These lesions were not routinely biopsied and most metastatic lesions were chemosensitive and radiosensitive. Our confirmation was inevitably based on observation of the clinical course.

Table 2 Disagreement between FDG-PET and conventional staging procedures (regional lymph node metastases)

Patient no.	Age (years)	Gender	CT N	PET N	PET M	Interval between CT scan of the chest and FDG-PET (days)	Comments
1	63	Male	3	3	0	8	Contralateral supraclavicular lymph node metastasis (PET)
5	64	Female	1	2	0	34	Subcarinal lymph node metastasis (PET)
16	71	Male	3	3	0	7	Contralateral supraclavicular lymph node metastasis (PET)
20	69	Male	3	3	0	20	Ipsilateral supraclavicular lymph node metastasis (PET)
25	60	Male	3	3	0	27	Ipsilateral supraclavicular lymph node metastasis (PET)
30	66	Male	2	2	0	7	Pretracheal lymph node metastasis (PET)
33	72	Male	3	3	0	13	Ipsilateral supraclavicular lymph node metastasis (PET)
41	49	Female	3	3	0	19	Contralateral supraclavicular lymph node metastasis (PET)
43	73	Male	2	0	0	34	False-positive pretracheal lymph node metastasis (CT)
56	48	Female	3	3	0	11	Ipsilateral supraclavicular lymph node metastasis (PET)
61	74	Male	2	0	0	27	False-positive superior mediastinal and subcarinal lymph nodes (CT).

FDG, fluorodeoxyglucose; PET, positron emission tomography; CT, computed tomography; N, node; M, metastasis.

We employed no special strategies to reduce the bias of PET readers. PET readers might have reported in such a way as to reduce or increase the impact of PET. One-third of patients received FDG-PET after commencement of chemotherapy. However, the median interval between commencement of chemotherapy and FDG-PET was 4 days (range: 1–11 days). We considered the chemotherapy to have had no effects on the findings of FDG-PET in such a short time after the initiation of chemotherapy.

FDG-PET is expected to have the potentially to both up- and downstage patients with SCLC as well as NSCLC. A previous study demonstrated that FDG-PET correctly downstaged ED to LD in three of 120 patients with SCLC [10]. These three patients had adrenal swelling on CT scan, but these lesions were negative on FDG-PET. On the other hand, FDG-PET correctly upstaged LD to ED in 10 of 120 patients with SCLC. It seems that SCLC seldom has a solitary distant metastasis because of its aggressive clinical behaviour. Most ED-SCLC has multiple, not solitary, or obvious distant metastasis. Furthermore, the health insurance system does not allow patients who obviously have metastatic lung cancer to receive FDG-PET in Japan. Therefore, we did not include patients with ED-SCLC in our analysis. Needless to say, FDG-PET is considered to be useful in patients with possible, but not evident, distant metastasis on other imaging tests, such as a solitary adrenal swelling.

According to the VALSG system, LD-SCLC is defined as a tumour confined to one hemithorax and regional lymph nodes [1]. Contralateral hilar or contralateral supraclavicular nodal involvement was classified as ED. According to the International Association for the Study of Lung Cancer (IASLC) consensus report, the classification of LD-SCLC includes bilateral hilar and/or supraclavicular nodal involvement, and ipsilateral pleural effusion [18]. A previous retrospective study demonstrated that the IASLC staging criteria for SCLC patients had a higher prognostic impact than VALSG criteria [19]. Therefore, we adopted the IASLC staging criteria for SCLC in our study.

In conclusion, FDG-PET scans detected unsuspected distant metastases in five of 63 patients with LD-SCLC (95% CI: 3–18%) and these findings resulted in a change of therapeutic strategies in these five patients. FDG-PET scans also detected contralateral supraclavicular lymph node metastases that had been negative on CT scans in three other

patients. These additional findings facilitated setting appropriate irradiation fields. FDG-PET scan is recommended as an initial staging tool in patients with apparent LD-SCLC.

Conflict of interest

The authors certify that there are no potential conflicts of interest.

Acknowledgments

We thank Takashi Sato, R.T., Hideaki Kitamura, R.T., Kazumasa Inoue, R.T. and Akira Hirayama, R.T. and Yoshiki Kojima, Ph.D. for technical assistance. This work was supported in part by a Grant from the Ministry of Health, Labour, and Welfare for the third term Comprehensive Strategy for Cancer Control and a Grant-in-Aid for Cancer Research from the Ministry of Health, Labour, and Welfare, Japan.

References

[1] Zelen M. Keynote address on biostatistics and data retrieval. Cancer Chemother Rep 1973;3(4):31–42.

[2] Takada M, Fukuoka M, Kawahara M, Sugiura T, Yokoyama A, Yokota S, et al. Phase III study of concurrent versus sequential thoracic radiotherapy in combination with cisplatin and etoposide for limited-stage small-cell lung cancer: results of the Japan Clinical Oncology Group Study 9104. J Clin Oncol 2002;20:3054–60.

[3] Turrisi 3rd AT, Kim K, Blum R, Sause WT, Livingston RB, Komaki R, et al. Twice-daily compared with once-daily thoracic radiotherapy in limited small-cell lung cancer treated concurrently with cisplatin and etoposide. N Engl J Med 1999;340:265–71.

[4] Noda K, Nishiwaki Y, Kawahara M, Negoro S, Sugiura T, Yokoyama A, et al. Irinotecan plus cisplatin compared with etoposide plus cisplatin for extensive small-cell lung cancer. N Engl J Med 2002;346:85–91.

[5] Pfister DG, Johnson DH, Azzoli CG, Sause W, Smith TJ, Baker Jr S, et al. American Society of Clinical Oncology treatment of unresectable non-small-cell lung cancer guideline: update 2003. J Clin Oncol 2004;22:330–53.

[6] MacManus MP, Hicks RJ, Matthews JP, Hogg A, McKenzie AF, Wirth A, et al. High rate of detection of unsuspected distant metastases by pet in apparent stage III non-small-cell lung cancer: implications for radical radiation therapy. Int J Radiat Oncol Biol Phys 2001;50:287–93.

[7] Eschmann SM, Friedel G, Paulsen F, Reimold M, Hehr T, Scheiderbauer J, et al. Impact of staging with ^{18}F-FDG-PET on outcome of patients with stage III non-small cell lung cancer: PET identifies potential survivors. Eur J Nucl Med Mol Imaging 2007;34:54–9.

[8] Kalff V, Hicks RJ, MacManus MP, Binns DS, McKenzie AF, Ware RE, et al. Clinical impact of ^{18}F fluorodeoxyglucose positron emission tomography in patients with non-small-cell lung cancer: a prospective study. J Clin Oncol 2001;19:111–8.

[9] Bradley JD, Dehdashti F, Mintun MA, Govindan R, Trinkaus K, Siegel BA. Positron emission tomography in limited-stage small-cell lung cancer: a prospective study. J Clin Oncol 2004;22:3248–54.

[10] Brink I, Schumacher T, Mix M, Ruhland S, Stoelben E, Digel W, et al. Impact of [^{18}F]FDG-PET on the primary staging of small-cell lung cancer. Eur J Nucl Med Mol Imaging 2004;31:1614–20.

[11] Blum R, MacManus MP, Rischin D, Michael M, Ball D, Hicks RJ. Impact of positron emission tomography on the management of patients with small-cell lung cancer: preliminary experience. Am J Clin Oncol 2004;27:164–71.

[12] Chin Jr R, McCain TW, Miller AA, Dunagan DP, Acostamadiedo J, Douglas Case L, et al. Whole body FDG-PET for the evaluation and staging of small cell lung cancer: a preliminary study. Lung Cancer 2002;37:1–6.

[13] Hauber HP, Bohuslavizki KH, Lund CH, Fritscher-Ravens A, Meyer A, Pforte A. Positron emission tomography in the staging of small-cell lung cancer: a preliminary study. Chest 2001;119:950–4.

[14] Kamel EM, Zwahlen D, Wyss MT, Stumpe KD, von Schulthess GK, Steinert HC. Whole-body ^{18}F-FDG PET improves the management of patients with small cell lung cancer. J Nucl Med 2003;44:1911–7.

[15] Pandit N, Gonen M, Krug L, Larson SM. Prognostic value of [^{18}F]FDG-PET imaging in small cell lung cancer. Eur J Nucl Med Mol Imag 2003;30:78–84.

[16] Schumacher T, Brink I, Mix M, Reinhardt M, Herget G, Digel W, et al. FDG-PET imaging for the staging and follow-up of small cell lung cancer. Eur J Nucl Med 2001;28:483–8.

[17] Shen YY, Shiau YC, Wang JJ, Ho ST, Kao CH. Whole-body 18F-2-deoxyglucose positron emission tomography in primary staging small cell lung cancer. Anticancer Res 2002;22:1257–64.

[18] Stahel RA, Ginsberg R, Havemann K, Hirsch FR, Ihde DC, Jassem J, et al. Staging and prognostic factors in small cell lung cancer: a consensus report. Lung Cancer 1989;5:119–26.

[19] Micke P, Faldum A, Metz T, Beeh KM, Bittinger F, Hengstler JG, et al. Staging small cell lung cancer: veterans administration lung study group versus international association for the study of lung cancer—what limits limited disease? Lung Cancer 2002;37:271–6.

Differential Constitutive Activation of the Epidermal Growth Factor Receptor in Non–Small Cell Lung Cancer Cells Bearing *EGFR* Gene Mutation and Amplification

Takafumi Okabe,[1] Isamu Okamoto,[1] Kenji Tamura,[3] Masaaki Terashima,[1] Takeshi Yoshida,[1] Taroh Satoh,[1] Minoru Takada,[2] Masahiro Fukuoka,[1] and Kazuhiko Nakagawa[1]

[1]Department of Medical Oncology, Kinki University School of Medicine; [2]National Kinki Central Chest Medical Center, Osaka, Japan; and [3]Department of Medical Oncology, Nara Hospital, Kinki University School of Medicine, Nara, Japan

Abstract

The identification of somatic mutations in the tyrosine kinase domain of the epidermal growth factor receptor (EGFR) in patients with non–small cell lung cancer (NSCLC) and the association of such mutations with the clinical response to EGFR tyrosine kinase inhibitors (TKI), such as gefitinib and erlotinib, have had a substantial effect on the treatment of this disease. *EGFR* gene amplification has also been associated with an increased therapeutic response to EGFR-TKIs. The effects of these two types of *EGFR* alteration on EGFR function have remained unclear, however. We have now examined 16 NSCLC cell lines, including eight newly established lines from Japanese NSCLC patients, for the presence of *EGFR* mutations and amplification. Four of the six cell lines that harbor *EGFR* mutations were found to be positive for *EGFR* amplification, whereas none of the 10 cell lines negative for *EGFR* mutation manifested *EGFR* amplification, suggesting that these two types of *EGFR* alteration are closely associated. Endogenous EGFRs expressed in NSCLC cell lines positive for both *EGFR* mutation and amplification were found to be constitutively activated as a result of ligand-independent dimerization. Furthermore, the patterns of both *EGFR* amplification and EGFR autophosphorylation were shown to differ between cell lines harboring the two most common types of *EGFR* mutation (exon 19 deletion and L858R point mutation in exon 21). These results reveal distinct biochemical properties of endogenous mutant forms of EGFR expressed in NSCLC cell lines and may have implications for treatment of this condition. [Cancer Res 2007;67(5):2046–53]

Introduction

The epidermal growth factor receptor (EGFR) is a 170-kDa transmembrane glycoprotein with an extracellular ligand binding domain, a transmembrane region, and a cytoplasmic tyrosine kinase domain and is encoded by a gene (*EGFR*) located at human chromosomal region 7p12 (1–3). The binding of ligand to EGFR induces receptor dimerization and consequent conformational changes that result in activation of the intrinsic tyrosine kinase, receptor autophosphorylation, and activation of a signaling cascade (4, 5). Aberrant signaling by EGFR plays an important role in cancer development and progression (3).

Requests for reprints: Isamu Okamoto, Department of Medical Oncology, Kinki University School of Medicine, 377-2, Ohno-higashi, Osaka-Sayama, Osaka 589-8511, Japan. Phone: 81-72-366-0221; Fax: 81-72-360-5000; E-mail: okamoto@dotd.med.kindai.ac.jp.

doi:10.1158/0008-5472.CAN-06-3339

EGFR is frequently overexpressed in non–small cell lung cancer (NSCLC) and has been implicated in the pathogenesis of this disease (6, 7). Given the biological importance of EGFR signaling in cancer, several agents have been synthesized that inhibit the receptor tyrosine kinase activity. Two such inhibitors of the tyrosine kinase activity of EGFR (EGFR-TKI), gefitinib and erlotinib, both of which compete with ATP for binding to the tyrosine kinase pocket of the receptor, have been extensively studied in patients with NSCLC (8, 9). We and others have shown that a clinical response to these agents is more common in women than in men, in Japanese than in individuals from Europe or the United States, in patients with adenocarcinoma than in those with other histologic subtypes of cancer, and in patients who have never smoked than in those with a history of smoking (10–14). Mutations in the tyrosine kinase domain of EGFR have also been detected in a subset of lung cancer patients and shown to predict sensitivity to EGFR-TKIs (15–17). Indeed, the clinical characteristics of patients with known *EGFR* mutations are similar to those of other individuals most likely to respond to treatment with EGFR-TKIs (18–22). These mutations arise in the first four exons (exons 18–21) corresponding to the tyrosine kinase domain of EGFR, and they affect key amino acids surrounding the ATP-binding cleft (23, 24). In-frame deletions that eliminate four highly conserved amino acids (LREA) encoded by exon 19 are the most common type of *EGFR* mutation, with missense point mutations in exon 21 that result in a specific amino acid substitution at position 858 (L858R) being the second most common. In addition to *EGFR* mutations, other molecular changes may play a role in determining sensitivity to EGFR-TKIs (22, 25–28). NSCLC patients with an increased *EGFR* copy number, as revealed by fluorescence *in situ* hybridization (FISH), have thus been found to show an increased response rate to and prolonged survival after gefitinib therapy (22, 25–27).

Given that *EGFR* is mutated or amplified (or both) in NSCLC, it is important to determine the biological effects of such *EGFR* alterations on EGFR function (15, 29–32). Transient transfection of various cell types with vectors encoding wild-type or mutant versions of EGFR showed that the activation of mutant receptors by EGF is more pronounced and sustained than is that of the wild-type receptor (15, 30). However, detailed biochemical analysis of NSCLC cell lines with endogenous *EGFR* mutations has been limited. We have now identified *EGFR* mutations in three NSCLC cell lines newly established from Japanese patients. Furthermore, we have characterized a panel of 16 NSCLC cell lines for *EGFR* mutations and amplification and evaluated the relation between the presence of these two types of *EGFR* alteration and sensitivity to gefitinib. The effects of *EGFR* alterations on activation status of EGFR and on downstream signaling were also evaluated.

Finally, in *EGFR* mutant cell lines showing constitutive EGFR activation, we assessed how the mutations activate the tyrosine kinase domain of the receptor.

Materials and Methods

Cell lines. The human NSCLC cell lines NCI-H226 (H226), NCI-H292 (H292), NCI-H460 (H460), NCI-H1299 (H1299), NCI-H1650 (H1650), and NCI-H1975 (H1975) were obtained from the American Type Culture Collection (Manassas, VA). PC-9 and A549 cells were obtained as described previously (33). Ma-1 cells were kindly provided by E. Shimizu (Tottori University, Yonago, Japan). We established seven cell lines (KT-2, KT-4, Ma-25, Ma-31, Ma-34, Ma-45, and Ma-53) from tissue or pleural effusion of Japanese patients with advanced NSCLC. These cell lines were cultured under a humidified atmosphere of 5% CO_2 at 37°C in RPMI 1640 (Sigma, St. Louis, MO) supplemented with 10% fetal bovine serum. Informed consent for establishment of cell lines and tumor DNA sequencing was obtained in accordance with the ethical guidelines for human genome/genetic analysis in Japan.

Growth inhibition assay. Gefitinib was kindly provided by AstraZeneca (Macclesfield, United Kingdom) as a pure substance and was diluted in DMSO to obtain a stock solution of 20 mmol/L. For growth inhibition assays, cells (0.5×10^4 to 4.5×10^4) were plated in 96-well flat-bottomed plates and cultured for 24 h before the addition of various concentrations of gefitinib and incubation for an additional 72 h. TetraColor One (5 mmol/L tetrazolium monosodium salt and 0.2 mmol/L 1-methoxy-5-methyl phenazinium methylsulfate; Seikagaku, Tokyo, Japan) was then added to each well, and the cells were incubated for 3 h at 37°C before measurement of absorbance at 490 nm with a Multiskan Spectrum instrument (Thermo Labsystems, Boston, MA). Absorbance values were expressed as a percentage of that for untreated cells, and the concentration of gefitinib resulting in 50% growth inhibition (IC_{50}) was calculated.

Genetic analysis of *EGFR*. Genomic DNA was extracted from cell lines with the use of a QIAamp DNA Mini kit (Qiagen, Tokyo, Japan), and exons 18 to 21 of *EGFR* were amplified by the PCR and sequenced directly. PCR was done in a reaction mixture (25 μL) containing 50 ng of genomic DNA and TaKaRa Taq polymerase (TaKaRa BIO, Tokyo, Japan) and with an initial incubation for 3 min at 94°C followed by 30 cycles of 20 s at 94°C, 30 s at 58°C, and 20 s at 72°C and by a final incubation for 7 min at 72°C. The PCR products were purified with a Microcon YM-100 filtration device (Millipore, Billerica, MA) before sequencing with the use of an ABI BigDye Terminator v. 3.1 Cycle Sequencing kit (Applied Biosystems, Foster City, CA). Sequencing reaction mixtures were subjected to electrophoresis with an ABI PRISM 3100 Genetic Analyzer (Applied Biosystems). Primers for mutation analysis (sense and antisense, respectively) were as follows: exon 18, 5′-CAAATGAGCTGGCAAGTGCCGTGTC-3′ and 5′-GAGTTTCC-CAAACACTCAGTGAAA-C-3′; exon 19, 5′-GCAATATCAGCCTTAGGT-GCGGCTC-3′and 5′-CATAGAAAGTGAACATTTAGGATGTG-3′; exon 20, 5′-CCATGAGTACGTATTTTGAAACTC-3′ and 5′-CATATCCCCATGG-CAAACTCTTGC-3′; and exon 21, 5′-CTAACGTTCGCCAGCCATAAGTCC-3′ and 5′-GCTGCGAGCTCACCCAGAATGTCTGG-3′.

FISH. *EGFR* copy number per cell was determined by FISH with the use of the LSI EGFR Spectrum Orange and CEP7 Spectrum Green probes (Vysis; Abbott, Des Plaines, IL). Cells were centrifuged onto glass slides with a Shandon cytocentrifuge (Thermo Electron, Pittsburgh, PA) and fixed by consecutive incubations with ice-cold 70% ethanol for 10 min, 85% ethanol for 5 min, and 100% ethanol for 5 min. Slides were stored at −20°C until analysis. Cells were subsequently subjected to digestion with pepsin for 10 min at 37°C, washed with water, dehydrated with a graded series of ethanol solutions, denatured with 70% formamide in 2× SSC for 5 min at 72°C, and dehydrated again with a graded series of ethanol solutions before incubation with a hybridization mixture consisting of 50% formamide, 2× SSC, Cot-1 DNA, and labeled DNA. The slides were washed for 5 min at 73°C with 3× SSC, for 5 min at 37°C with 4× SSC containing 0.1% Triton X-100, and for 5 min at room temperature with 2× SSC before counterstaining with antifade solution containing 4′,6-diamidino-2-phenylindole. Hybridization signals were scored in 40 nuclei with the use of a ×100 immersion objective. Nuclei with a disrupted boundary were excluded from the analysis. Gene amplification was defined by an *EGFR*/chromosome 7 copy number ratio of ≥2 or by the presence of clusters of ≥15 copies of *EGFR* per cell in ≥10% of cells, as described previously (25, 27).

Immunoblot analysis. Cell lysates were fractionated by SDS-PAGE on a 7.5% gel, and the separated proteins were transferred to a nitrocellulose membrane. After blocking of nonspecific sites with 5% skim milk, the membrane was incubated overnight at room temperature with primary antibodies. Antibodies to phosphorylated EGFR (pY845, pY1068, or pY1173), extracellular signal-regulated kinase (ERK), phosphorylated AKT, AKT, Src homology and collagen (Shc), and phosphorylated Shc were obtained from Cell Signaling Technology (Beverly, MA); antibodies to EGFR were from Zymed (South San Francisco, CA); antibodies to phosphorylated ERK were from Santa Cruz Biotechnology (Santa Cruz, CA); and antibodies to β-actin (loading control) were from Sigma. Immune complexes were detected by incubation of the membrane for 1 h at room temperature with horseradish peroxidase–conjugated goat antibodies to mouse or rabbit immunoglobulin (Amersham Biosciences, Little Chalfont, United Kingdom) and by subsequent exposure to enhanced chemiluminescence reagents (Perkin-Elmer, Boston, MA).

Table 1. Characteristics of NSCLC cell lines

Cell lines	Gefitinib IC_{50} (μmol/L)	*EGFR* mutation	*EGFR* amplification	Histology
PC-9	0.07	del(E746-A750)	+	Adenocarcinoma
KT-2	0.57	L858R	+	Adenocarcinoma
KT-4	1.26	L858R	+	Large cell carcinoma
Ma-1	2.34	del(E746-A750)	+	Adenocarcinoma
H1650	6.66	del (E746-A750)	−	Adenocarcinoma
A549	8.70	Wild type	−	Adenocarcinoma
H1975	9.32	L858R+T790M	−	Adenocarcinoma
H292	9.44	Wild type	−	Mucoepidermoid carcinoma
H226	9.53	Wild type	−	Squamous cell carcinoma
Ma-25	10.17	Wild type	−	Large cell carcinoma
H460	10.38	Wild type	−	Large cell carcinoma
Ma-45	10.47	Wild type	−	Adenocarcinoma
Ma-53	10.47	Wild type	−	Adenocarcinoma
Ma-34	11.17	Wild type	−	Adenocarcinoma
H1299	11.28	Wild type	−	Large cell carcinoma
Ma-31	12.46	Wild type	−	Adenocarcinoma

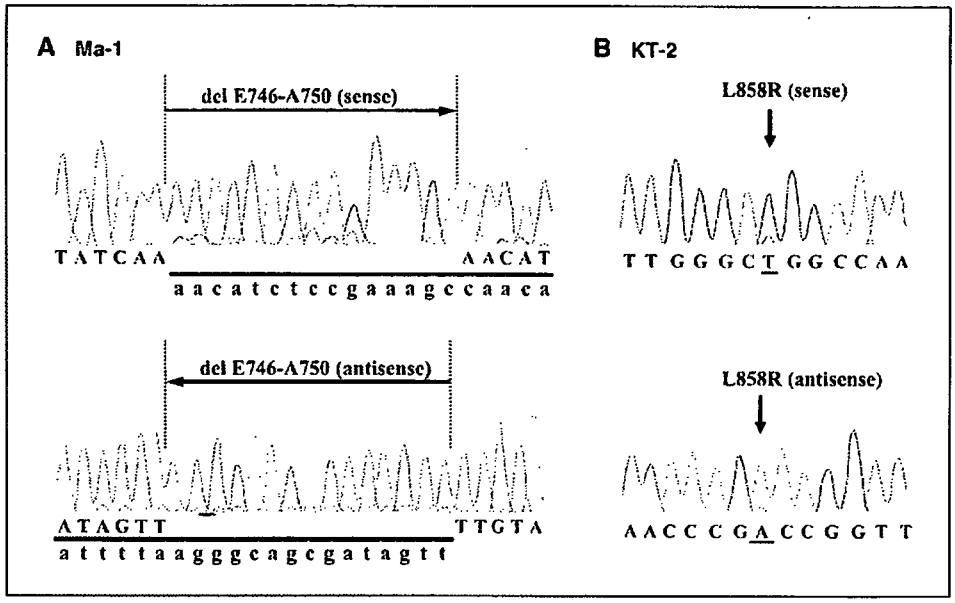

Figure 1. Detection of *EGFR* mutations in NSCLC cell lines. The portions of the sequencing electrophoretograms corresponding to the mutations are shown for Ma-1 (*A*) and KT-2 (*B*) cells. *A*, heterozygous in-frame deletion in exon 19 is revealed by the presence of double peaks. Tracings in both sense and antisense directions are shown to highlight the two breakpoints of the deletion. Wild-type (*uppercase*) and mutant (*lowercase*) nucleotide sequences. *B*, heterozygous point mutation (T — G) at nucleotide position 2819 in exon 21.

Treatment of cells with neutralizing antibodies. Cells were exposed to neutralizing antibodies (each at 12 μg/mL) for 3 h before EGF stimulation. The antibodies included those to EGF and to transforming growth factor-α (TGF-α), both from R&D Systems (Minneapolis, MN) as well as antibodies to EGFR (Upstate Biotechnology, Lake Placid, NY). Cell lysates were then prepared and subjected to immunoblot analysis with antibodies to phosphorylated EGFR (pY1068) and to EGFR as described above.

Chemical cross-linking assay. Chemical cross-linking was done as described previously (34, 35). Cells were washed twice with ice-cold PBS and then incubated for 20 min at 4°C with 1 mmol/L bis(sulfosuccinimidyl)-suberate (Pierce, Rockford, IL) in PBS. The cross-linking reaction was terminated by the addition of glycine to a final concentration of 250 mmol/L and incubation for an additional 5 min at 4°C. The cells were washed with PBS, and cell lysates were resolved by SDS-PAGE on a 4% gel and subjected to immunoblot analysis with anti-EGFR (Santa Cruz Biotechnology).

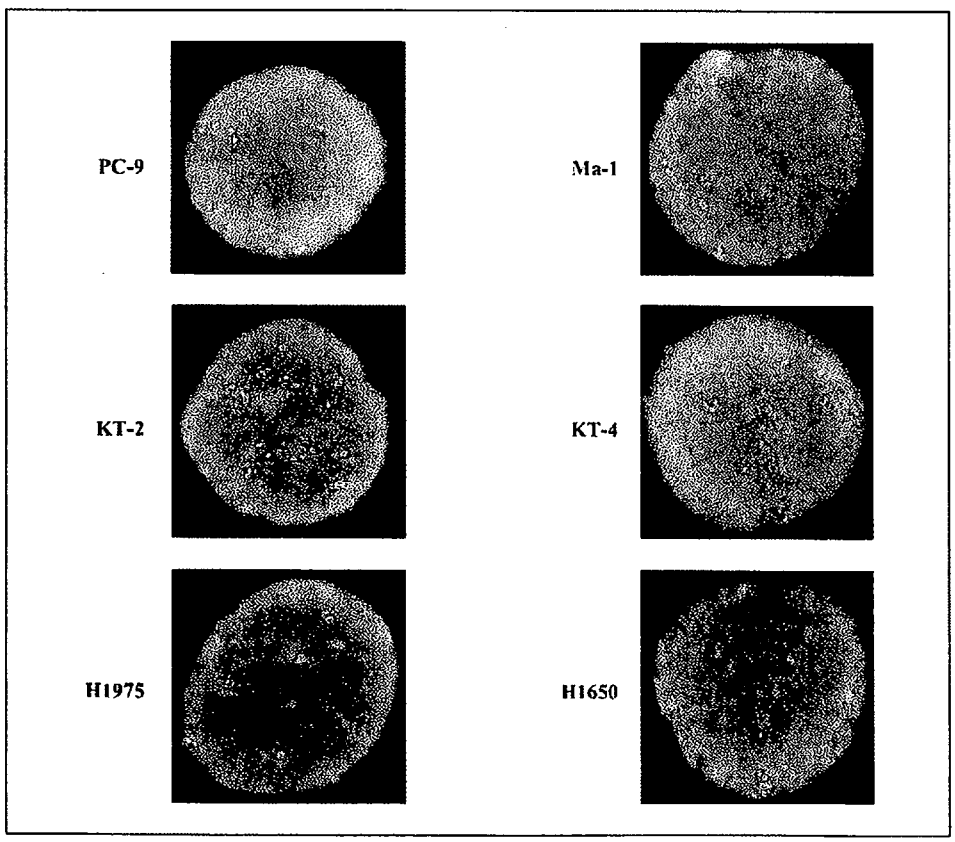

Figure 2. FISH analysis of *EGFR* amplification in NSCLC cell lines. The analysis was done with probes specific for *EGFR* (*red signals*) and for the centromere of chromosome 7 (*green signals*) in the indicated cell lines. PC-9 and Ma-1 cells manifest an *EGFR*/ chromosome copy number ratio of ≥2, whereas KT-2 and KT-4 cells manifest *EGFR* clusters. H1975 and H1650 cells are negative for *EGFR* amplification.

Results

Effect of gefitinib on the growth of NSCLC cell lines. We first examined the effect of the EGFR-TKI gefitinib on the growth of 16 NSCLC cell lines, eight of which (KT-2, KT-4, Ma-1, Ma-25, Ma-31, Ma-34, Ma-45, and Ma-53) were established from Japanese NSCLC patients for the present study. The IC_{50} values for gefitinib chemosensitivity ranged from 0.07 to 12.46 μmol/L (a 178-fold difference; Table 1).

Four cell lines (PC-9, KT-2, KT-4, and Ma-1) were relatively sensitive to gefitinib with IC_{50} values between 0.07 and 2.34 μmol/L, whereas the remaining 12 lines were considered resistant to gefitinib (IC_{50} > 6 μmol/L). No relation was apparent between sensitivity to gefitinib and histologic subtype of NSCLC for this panel of cell lines (Table 1).

***EGFR* mutation and amplification in NSCLC cell lines.** We screened the 16 NSCLC cell lines for the presence of *EGFR* mutations in exons 18 to 21, which encode the catalytic domain of the receptor. As previously described (36–39), PC-9, H1650, and H1975 cell lines were found to harbor *EGFR* mutations [del(E746-A750) in PC-9 and H1650 and both L858R and T790M in H1975]. Furthermore, we detected *EGFR* mutations in three of the newly established cell lines (Ma-1, KT-2, and KT-4). Ma-1 cells, which were isolated from a female ex smoker with adenocarcinoma (>30 years of age), were found to harbor a small deletion within exon 19 [del(E746-A750); Fig. 1*A*; Table 1]. Both KT-2 cells [derived from a male ex smoker with adenocarcinoma (>30 years of age)] and KT-4 cells (derived from a male nonsmoker with large cell carcinoma) harbor a point mutation (L858R) in exon 21 (Fig. 1*B*; Table 1). Four of these six NSCLC cell lines with *EGFR* mutations (PC-9, Ma-1, KT-2, and KT-4) are sensitive to gefitinib (Table 1), consistent with clinical observations (15–17, 20, 22).

We next examined the 16 NSCLC cell lines for the presence of *EGFR* amplification by FISH analysis with a probe specific for *EGFR* and a control probe for the centromere of chromosome 7. Four (PC-9, Ma-1, KT-2, and KT-4) of the 16 cell lines, all of which harbor *EGFR* mutations, were found to be positive for *EGFR* amplification (Fig. 2; Table 1). PC-9 and Ma-1 cell lines, both of which harbor the same exon 19 deletion, showed an *EGFR*/chromosome copy number ratio of ≥2, whereas KT-2 and KT-4, both of which harbor the L858R mutation in exon 21, showed a clustered unbalanced gain of *EGFR* copy number (Fig. 2). The four cell lines that manifested both *EGFR* mutation and amplification were sensitive to gefitinib (Table 1). The *EGFR* mutant cell lines H1650 and H1975 showed no evidence of *EGFR* amplification (Fig. 2), and both of these lines were relatively resistant to gefitinib (Table 1). None of the cell lines negative for *EGFR* mutations manifested *EGFR* amplification (Table 1), suggesting that *EGFR* mutation is closely associated with *EGFR* amplification ($P < 0.05$, χ^2 test).

EGFR expression in NSCLC cell lines. We examined the basal abundance of EGFR in *EGFR* wild-type and mutant NSCLC cell lines by immunoblot analysis. The amount of EGFR in the cell lines PC-9, Ma-1, KT-2, and KT-4, all of which manifest *EGFR* amplification and *EGFR* mutation, was increased compared with that in *EGFR* wild-type cell lines (A549 and H1299) or *EGFR* mutant cell lines negative for *EGFR* amplification (H1975 and H1650; Fig. 3). These results, thus, reveal a close relation between increased EGFR expression and *EGFR* amplification in this panel of NSCLC cell lines, consistent with the results of previous analyses of NSCLC tissue specimens (6, 7).

EGFR phosphorylation in NSCLC cell lines. We examined tyrosine phosphorylation of endogenous EGFRs in NSCLC cell lines by immunoblot analysis with phosphorylation site–specific antibodies. In cells (A549) that express only wild-type EGFR, phosphorylation of the receptor at Y845, Y1068, or Y1173 was undetectable in the absence of EGF but was markedly induced on

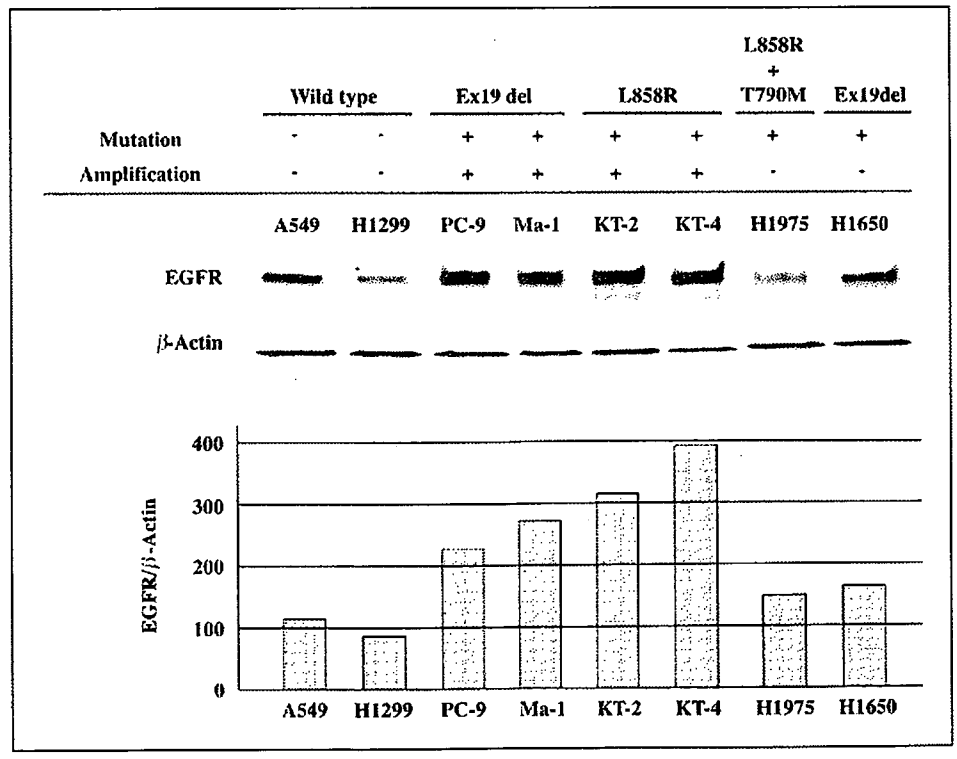

Figure 3. EGFR expression in NSCLC cell lines. Lysates (40 μg of protein) of NSCLC cell lines positive or negative for *EGFR* mutation or amplification, as indicated, were subjected to immunoblot analysis with antibodies to EGFR and to β-actin (*top*). The abundance of EGFR relative to that of β-actin was determined by densitometry (*bottom*). Representative of three independent experiments.

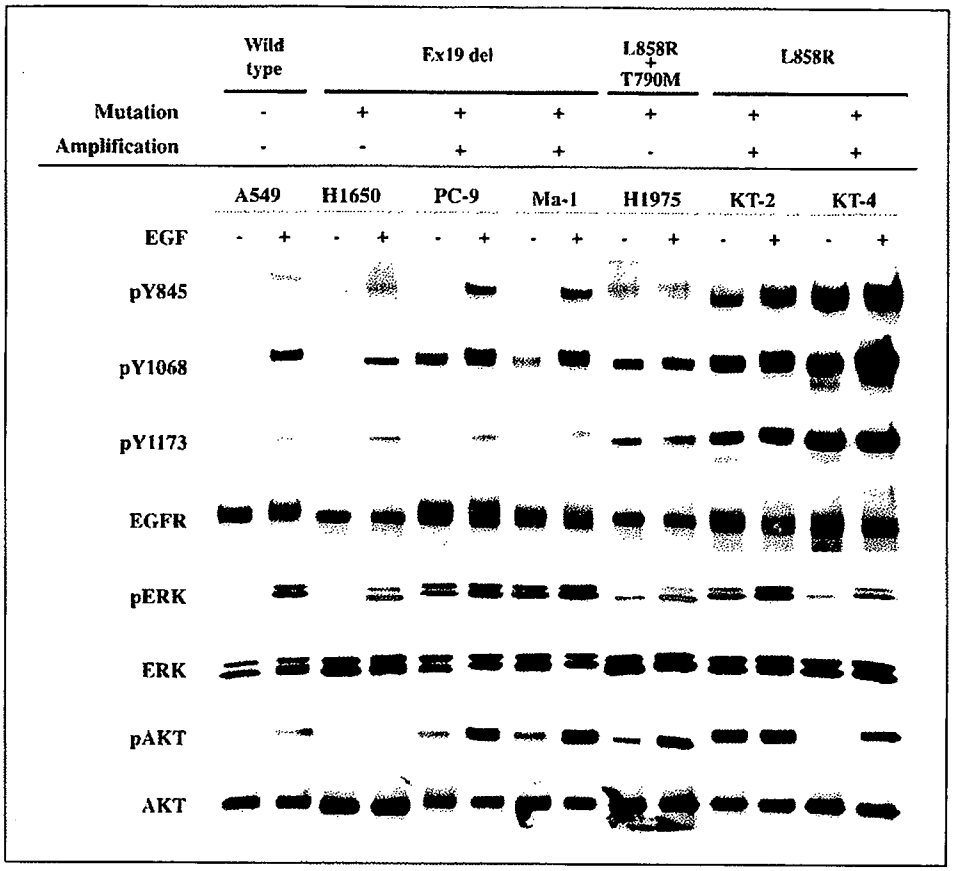

Figure 4. Phosphorylation of EGFR and downstream signaling molecules in NSCLC cell lines. Serum-deprived cells were incubated for 15 min in the absence or presence of EGF (100 ng/mL), after which cell lysates (40 μg of protein) were subjected to immunoblot analysis with antibodies to phosphorylated forms of EGFR (*pEGFR*), ERK (*pERK*), or AKT (*pAKT*) as well as antibodies to all forms of the corresponding proteins, as indicated. Representative of three independent experiments.

exposure of the cells to this growth factor (Fig. 4). Similar results were obtained with H1650 cells, which are positive for the deletion in exon 19 of *EGFR* but negative for *EGFR* amplification. In contrast, PC-9 and Ma-1 cells, which are positive for both the exon 19 deletion and *EGFR* amplification, manifested an increased basal level of EGFR phosphorylation at Y1068, indicative of constitutive activation of the EGFR tyrosine kinase. Exposure of PC-9 or Ma-1 cells to EGF induced EGFR phosphorylation at Y845 and Y1173, showing that the mutant receptors remain sensitive to ligand stimulation. Furthermore, the cell lines (H1975, KT-2, and KT-4) with the L858R point mutation manifested an increased basal level of EGFR phosphorylation at Y845, Y1068, and Y1173, and the extent of phosphorylation at these residues was increased only slightly by treatment of the cells with EGF, indicative of constitutive activation of the EGFR tyrosine kinase. These results thus showed that endogenous *EGFR* mutations result in constitutive receptor activation, and that the patterns of tyrosine phosphorylation of EGFR differ between the two most common types of *EGFR* mutant.

Phosphorylation of signaling molecules downstream of EGFR in NSCLC cell lines. Given that constitutive activation of EGFR was detected in NSCLC cell lines with endogenous *EGFR* mutations, we examined whether signaling molecules that act downstream of the receptor are also constitutively activated in these cell lines. We first examined the basal levels of phosphorylation of AKT and ERK, both of which mediate the oncogenic effects of EGFR. Immunoblot analysis with antibodies to phosphorylated forms of AKT or ERK revealed that these molecules are indeed constitutively activated in the *EGFR* mutant lines (PC-9, Ma-1, H1975, KT-2, and KT-4) that manifest constitutive activation of EGFR, although the extent of phosphorylation varied (Fig. 4). The increased levels of AKT and ERK phosphorylation in these mutant cell lines are consistent with the increased level of EGFR phosphorylation on Y1068, which serves as the docking site for phosphatidylinositol 3-kinase and growth factor receptor binding protein 2, molecules that mediate the activation of AKT and the Ras-ERK pathway, respectively (2, 40). We next examined whether the differences in the pattern of constitutive tyrosine phosphorylation of EGFR apparent between NSCLC cell lines harboring the exon 19 deletion and those with the L858R mutation in exon 21 are associated with distinct alterations in downstream signaling pathways. Given that Y1173, a major docking site of EGFR for the adapter protein Shc (2, 40, 41), is constitutively phosphorylated in cells with the L858R mutation but not in those with the exon 19 deletion, we compared Shc phosphorylation between cell lines with these two types of *EGFR* mutation. Ligand-independent tyrosine phosphorylation of the 52- and 46-kDa isoforms of Shc was apparent in cell lines with either type of *EGFR* mutation (Fig. 5). However, cell lines (KT-2 and KT-4) that harbor the L858R mutation exhibited a markedly greater basal level of phosphorylation of the 66-kDa isoform of Shc than did those (PC-9 and Ma-1) that harbor the exon 19 deletion or those (A549) that harbor only wild-type *EGFR*. These data suggest that the constitutively active mutant forms of *EGFR* induce selective activation of downstream effectors as a result of differential patterns of receptor autophosphorylation.

Ligand-independent dimerization and activation of *EGFR* mutants. Evidence suggests that EGFR ligands, including EGF and TGF-α, secreted by tumor cells themselves might be responsible for activation of mutant receptors in an autocrine loop (29, 42). To investigate whether EGFR is constitutively activated as a result of such an autocrine mechanism in *EGFR* mutant NSCLC cell lines, we treated the cells with a combination of three neutralizing antibodies (anti-EGF, anti-TGF-α, and anti-EGFR) for 3 h and then examined the effect of EGF on EGFR phosphorylation. The ligand-dependent activation of EGFR in A549 cells (which express only wild-type *EGFR*) was blocked by such antibody treatment (Fig. 6*A*). In contrast, treatment of the *EGFR* mutant cell lines PC-9 or KT-4 with the neutralizing antibodies failed to inhibit the constitutive phosphorylation of EGFR on Y1068. These observations suggest that the constitutive phosphorylation of the mutant receptors is not attributable to autocrine stimulation, although we are not able to exclude a possible role for other EGFR ligands.

Ligand-induced EGFR dimerization is responsible for activation of the receptor tyrosine kinase (4, 5). To determine whether mutant receptors are constitutively dimerized, we treated *EGFR* wild-type or mutant cell lines with a cross-linking agent before immunoblot analysis with antibodies to EGFR. Whereas ligand-induced dimerization of wild-type *EGFR* was observed in A549 cells, receptor dimerization in PC-9 and KT-4 cells, which express mutant receptors, was apparent in the absence of ligand and was not increased substantially by exposure of the cells to EGF (Fig. 6*B*). These data indicate that ligand-independent receptor dimerization is responsible for the constitutive activation of the mutant forms of *EGFR*.

Discussion

The discovery of somatic mutations in the tyrosine kinase domain of EGFR and of their association with a high response rate to EGFR-TKIs has had a substantial effect on the treatment of advanced NSCLC (15–17, 20, 22). Asian patients with NSCLC seem to have a higher prevalence of these mutations, ranging from 20% to 40% (18, 20, 21, 43–45). We have now identified *EGFR* mutations in three of eight newly established cell lines from Japanese patients with advanced NSCLC. Characterization of these eight new cell lines and eight previously established NSCLC lines revealed that, consistent with previous observations (29, 31, 36), those cell lines that harbor *EGFR* mutations are more likely to be sensitive to gefitinib than are those without such mutations. Not all *EGFR* mutant cell lines (e.g., H1650 and H1975) are sensitive to this EGFR-TKI, however, suggesting the existence of additional determinants of gefitinib sensitivity. In addition to the L858R mutation in exon 21 of *EGFR*, H1975 cells contain the T790M mutation in exon 20, which has been shown to confer resistance to EGFR-TKIs (38, 39). H1650 cells, which do not harbor mutations in *EGFR* other than the exon 19 deletion, manifest loss of the tumor suppressor phosphatase and tensin homologue deleted on chromosome 10 (37), which may result in resistance to EGFR-TKIs. *EGFR* amplification in NSCLC cells has also been shown to correlate with a better response to gefitinib (22, 25–27). Given that little is known of the relation between *EGFR* mutation and amplification in NSCLC, we examined the 16 NSCLC cell lines used in this study for *EGFR* amplification by FISH. Four of the six cell lines with *EGFR* mutations were found to be positive for gene amplification, whereas none of the 10 mutation-negative cell lines manifested *EGFR* amplification. This finding thus suggests that *EGFR* mutation and amplification are linked. Cappuzzo et al. showed that 6 of 9 (67%) NSCLC patients with *EGFR* amplification also had *EGFR* mutations (25). Furthermore, Takano et al. sequenced *EGFR* and determined the *EGFR* copy number by real-time PCR analysis for the tumors of 66 NSCLC patients (22); all of the patients with a high *EGFR* copy number (≥6.0 per cell) also had *EGFR* mutations. Moreover, PCR analysis revealed selective amplification of the mutant *EGFR* alleles in the patients with a high *EGFR* copy number. Our sequencing electrophoretograms for the *EGFR* mutant cell lines positive for *EGFR* amplification also revealed that the mutant signals were dominant, and the wild-type sequence was barely detectable (Fig. 1), indicative of selective amplification of the mutant alleles. We used the recently proposed definition of *EGFR* amplification as determined by FISH (25, 27) and found that the pattern of gene amplification seemed to be dependent on the

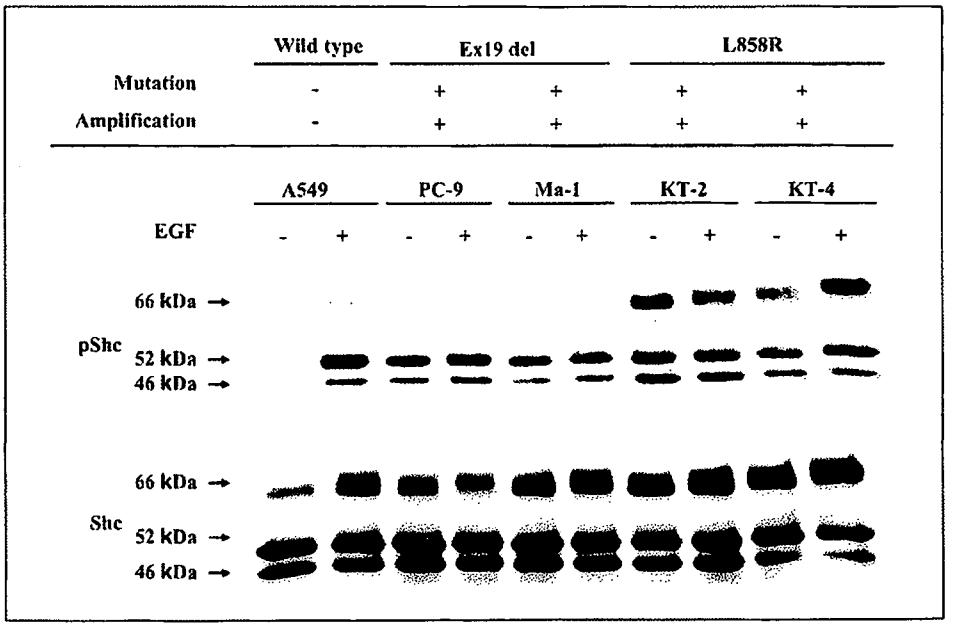

Figure 5. Phosphorylation of Shc in NSCLC cell lines. Serum-deprived cells were incubated for 15 min in the absence or presence of EGF (100 ng/mL), after which cell lysates (40 μg of protein) were subjected to immunoblot analysis with antibodies to phosphorylated Shc (*pShc*) or total Shc. Representative of three independent experiments.

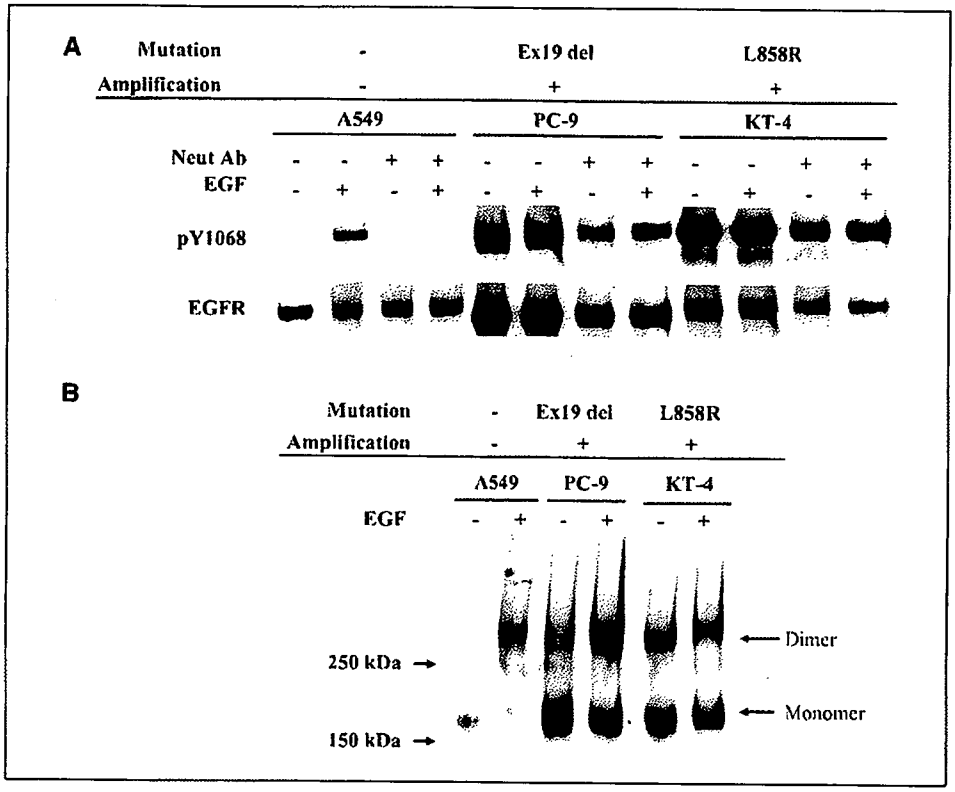

Figure 6. Mechanism of constitutive activation of EGFR in NSCLC cell lines. *A*, effect of neutralizing antibodies (*Neut Ab*) on EGFR phosphorylation. Serum-deprived NSCLC cells (A549, PC-9, or KT-4) were incubated for 3 h with a combination of neutralizing antibodies to EGF, TGF-α, and EGFR and then for 15 min in the additional absence or presence of EGF (100 ng/mL). Cell lysates were then prepared and subjected to immunoblot analysis with antibodies to the Y1068-phosphorylated form of EGFR or to total EGFR. *B*, EGFR dimerization. Serum-deprived cells were incubated for 15 min in the absence or presence of EGF (100 ng/mL), exposed to a chemical cross-linker, lysed, and subjected to immunoblot analysis with antibodies to EGFR. Representative of three independent experiments.

type of *EGFR* mutation; gene clusters were observed in cells with the L858R mutation in exon 21, whereas an *EGFR*/chromosome copy number ratio of ≥2 was detected in those with the small deletion [del(E746-A750)] in exon 19. Together, these data support the notion that *EGFR* mutation and amplification may be co-selected for during the growth of NSCLC cells. The four cell lines (PC-9, Ma-1, KT-2, and KT-4) positive for both *EGFR* mutation and amplification were sensitive to gefitinib, suggesting that *EGFR* amplification may increase sensitivity to gefitinib in *EGFR* mutant cells.

Previous biochemical studies of cells transiently transfected with vectors for wild-type or mutant forms of EGFR suggested that *EGFR* mutations increase EGF-dependent receptor activation (15, 30). Infection of NIH 3T3 cells with a retrovirus encoding *EGFR* mutants showed that the mutant receptors are constitutively activated and able to induce cell transformation in the absence of exogenous EGF (32). We examined the activation status of endogenous EGFRs in the six NSCLC cell lines that harbor *EGFR* mutations. The H1650, PC-9, and Ma-1 cell lines, all of which harbor the same exon 19 deletion, showed different patterns of EGFR autophosphorylation in the COOH-terminal region of the protein. EGFR autophosphorylation was ligand dependent in H1650 cells, which are negative for *EGFR* amplification, whereas Y1068 (but not Y845 and Y1173) was constitutively phosphorylated in PC-9 and Ma-1 cells, both of which manifest *EGFR* amplification. These results suggest that both *EGFR* mutation and amplification may be required for constitutive activation of EGFR in NSCLC cells that harbor the exon 19 deletion. In contrast, NSCLC cell lines (H1975, KT-2, and KT-4) that harbor the L858R mutation exhibited constitutive phosphorylation of EGFR at Y845, Y1068, and Y1173, regardless of the absence or presence of *EGFR* amplification. It is thought that *EGFR* mutations result in repositioning of critical residues surrounding the ATP-binding cleft of the tyrosine kinase domain of the receptor and thereby stabilize the interactions with ATP and EGF-TKIs, leading to increased tyrosine kinase activity and EGFR-TKI sensitivity (15, 23, 24). The differential activation of *EGFR* mutants observed in the present study may result from distinct conformational changes within the catalytic pocket caused by the different types of *EGFR* mutation. NSCLC patients with exon 19 deletions were recently shown to manifest longer overall survival than did those with the exon 21 point mutation after treatment with EGFR-TKIs, supporting the notion that the two major types of mutant receptors have different biological properties (46, 47).

Ligand-induced receptor dimerization underlies the activation of receptor tyrosine kinases (4, 5). Chemical cross-linking revealed that EGF binding to EGFR induced receptor dimerization in A549 cells, which express only the wild-type form of the receptor. In contrast, endogenous EGFRs in NSCLC cells harboring either the exon 19 deletion or the point mutation in exon 21 of *EGFR* were found to dimerize in the absence of ligand, suggesting that the constitutive activation of the mutant receptors is attributable to ligand-independent dimerization. EGFR dimerization was shown to be induced by interaction of quinazolines with the ATP-binding site of the receptor in the absence of ligand binding, suggesting that a change in conformation around the ATP-binding pocket of EGFR is sufficient for receptor dimerization (35). Conformational changes induced by *EGFR* mutations may therefore also trigger EGFR dimerization in *EGFR* mutant cells.

In conclusion, we have found that *EGFR* mutation is closely associated with *EGFR* amplification in NSCLC cell lines. Endogenous EGFRs expressed in NSCLC cells positive for both *EGFR* mutation and amplification are constitutively activated as a result

of ligand-independent dimerization. Cells with the two most common types of *EGFR* mutation also manifest different patterns of EGFR autophosphorylation. Prospective studies are required to determine the potential for exploitation of these *EGFR* alterations in the treatment of advanced NSCLC.

Acknowledgments

Received 9/12/2006; revised 10/30/2006; accepted 12/10/2006.

The costs of publication of this article were defrayed in part by the payment of page charges. This article must therefore be hereby marked *advertisement* in accordance with 18 U.S.C. Section 1734 solely to indicate this fact.

We thank Takeko Wada, Erina Hatashita, and Yuki Yamada for technical assistance.

References

1. Wang Y, Minoshima S, Shimizu N. Precise mapping of the EGF receptor gene on the human chromosome 7p12 using an improved FISH technique. Jpn J Hum Genet 1993;38:399–406.
2. Jorissen RN, Walker F, Pouliot N, Garrett TP, Ward CW, Burgess AW. Epidermal growth factor receptor: mechanisms of activation and signalling. Exp Cell Res 2003; 284:31–53.
3. Hynes NE, Lane HA. ERBB receptors and cancer: the complexity of targeted inhibitors. Nat Rev Cancer 2005; 5:341–54.
4. Ogiso H, Ishitani R, Nureki O, et al. Crystal structure of the complex of human epidermal growth factor and receptor extracellular domains. Cell 2002;110:775–87.
5. Schlessinger J. Ligand-induced, receptor-mediated dimerization and activation of EGF receptor. Cell 2002;110:669–72.
6. Hirsch FR, Varella-Garcia M, Bunn PA, Jr., et al. Epidermal growth factor receptor in non-small-cell lung carcinomas: correlation between gene copy number and protein expression and impact on prognosis. J Clin Oncol 2003;21:3798–807.
7. Suzuki S, Dobashi Y, Sakurai H, Nishikawa K, Hanawa M, Ooi A. Protein overexpression and gene amplification of epidermal growth factor receptor in nonsmall cell lung carcinomas. An immunohistochemical and fluorescence *in situ* hybridization study. Cancer 2005;103: 1265–73.
8. Shepherd FA, Rodrigues Pereira J, Ciuleanu T, et al. Erlotinib in previously treated non-small-cell lung cancer. N Engl J Med 2005;353:123–32.
9. Thatcher N, Chang A, Parikh P, et al. Gefitinib plus best supportive care in previously treated patients with refractory advanced non-small-cell lung cancer: results from a randomised, placebo-controlled, multicentre study (Iressa Survival Evaluation in Lung Cancer). Lancet 2005;366:1527–37.
10. Fukuoka M, Yano S, Giaccone G, et al. Multi-institutional randomized phase II trial of gefitinib for previously treated patients with advanced non-small-cell lung cancer (the IDEAL 1 trial). J Clin Oncol 2003;21: 2237–46.
11. Kaneda H, Tamura K, Kurata T, Uejima H, Nakagawa K, Fukuoka M. Retrospective analysis of the predictive factors associated with the response and survival benefit of gefitinib in patients with advanced non-small-cell lung cancer. Lung Cancer 2004;46:247–54.
12. Takano T, Ohe Y, Kusumoto M, et al. Risk factors for interstitial lung disease and predictive factors for tumor response in patients with advanced non-small cell lung cancer treated with gefitinib. Lung Cancer 2004;45:93–104.
13. Tamura K, Fukuoka M. Gefitinib in non-small cell lung cancer. Expert Opin Pharmacother 2005;6:985–93.
14. Ando M, Okamoto I, Yamamoto N, et al. Predictive factors for interstitial lung disease, antitumor response, and survival in non-small-cell lung cancer patients treated with gefitinib. J Clin Oncol 2006;24:2549–56.
15. Lynch TJ, Bell DW, Sordella R, et al. Activating mutations in the epidermal growth factor receptor underlying responsiveness of non-small-cell lung cancer to gefitinib. N Engl J Med 2004;350:2129–39.
16. Paez JG, Janne PA, Lee JC, et al. EGFR mutations in lung cancer: correlation with clinical response to gefitinib therapy. Science 2004;304:1497–500.
17. Pao W, Miller V, Zakowski M, et al. EGF receptor gene mutations are common in lung cancers from "never smokers" and are associated with sensitivity of tumors to gefitinib and erlotinib. Proc Natl Acad Sci U S A 2004; 101:13306–11.
18. Kosaka T, Yatabe Y, Endoh H, Kuwano H, Takahashi T, Mitsudomi T. Mutations of the epidermal growth factor receptor gene in lung cancer: biological and clinical implications. Cancer Res 2004; 64:8919–23.
19. Han SW, Kim TY, Hwang PG, et al. Predictive and prognostic impact of epidermal growth factor receptor mutation in non-small-cell lung cancer patients treated with gefitinib. J Clin Oncol 2005;23:2493–501.
20. Mitsudomi T, Kosaka T, Endoh H, et al. Mutations of the epidermal growth factor receptor gene predict prolonged survival after gefitinib treatment in patients with non-small-cell lung cancer with postoperative recurrence. J Clin Oncol 2005;23:2513–20.
21. Tokumo M, Toyooka S, Kiura K, et al. The relationship between epidermal growth factor receptor mutations and clinicopathologic features in non-small cell lung cancers. Clin Cancer Res 2005;11:1167–73.
22. Takano T, Ohe Y, Sakamoto H, et al. Epidermal growth factor receptor gene mutations and increased copy numbers predict gefitinib sensitivity in patients with recurrent non-small-cell lung cancer. J Clin Oncol 2005;23:6829–37.
23. Gazdar AF, Shigematsu H, Herz J, Minna JD. Mutations and addiction to EGFR: the Achilles 'heal' of lung cancers? Trends Mol Med 2004;10:481–6.
24. Shigematsu H, Gazdar AF. Somatic mutations of epidermal growth factor receptor signaling pathway in lung cancers. Int J Cancer 2006;118:257–62.
25. Cappuzzo F, Hirsch FR, Rossi E, et al. Epidermal growth factor receptor gene and protein and gefitinib sensitivity in non-small-cell lung cancer. J Natl Cancer Inst 2005;97:643–55.
26. Hirsch FR, Varella-Garcia M, McCoy J, et al. Increased epidermal growth factor receptor gene copy number detected by fluorescence *in situ* hybridization associates with increased sensitivity to gefitinib in patients with bronchioloalveolar carcinoma subtypes: a Southwest Oncology Group Study. J Clin Oncol 2005;23:6838–45.
27. Tsao MS, Sakurada A, Cutz JC, et al. Erlotinib in lung cancer: molecular and clinical predictors of outcome. N Engl J Med 2005;353:133–44.
28. Ishikawa N, Daigo Y, Takano A, et al. Increases of amphiregulin and transforming growth factor-α in serum as predictors of poor response to gefitinib among patients with advanced non-small cell lung cancers. Cancer Res 2005;65:9176–84.
29. Tracy S, Mukohara T, Hansen M, Meyerson M, Johnson BE, Janne PA. Gefitinib induces apoptosis in the EGFRL858R non-small-cell lung cancer cell line H3255. Cancer Res 2004;64:7241–4.
30. Sordella R, Bell DW, Haber DA, Settleman J. Gefitinib-sensitizing EGFR mutations in lung cancer activate anti-apoptotic pathways. Science 2004;305:1163–7.
31. Amann J, Kalyankrishna S, Massion PP, et al. Aberrant epidermal growth factor receptor signaling and enhanced sensitivity to EGFR inhibitors in lung cancer. Cancer Res 2005;65:226–35.
32. Greulich H, Chen TH, Feng W, et al. Oncogenic transformation by inhibitor-sensitive and -resistant EGFR mutants. PLoS Med 2005;2:1167–76.
33. Yonesaka K, Tamura K, Kurata T, et al. Small interfering RNA targeting survivin sensitizes lung cancer cell with mutant p53 to Adriamycin. Int J Cancer 2006; 118:812–20.
34. Koizumi F, Shimoyama T, Taguchi F, Saijo N, Nishio K. Establishment of a human non-small cell lung cancer cell line resistant to gefitinib. Int J Cancer 2005;116:36–44.
35. Arteaga CL, Ramsey TT, Shawver LK, Guyer CA. Unliganded epidermal growth factor receptor dimerization induced by direct interaction of quinazolines with the ATP binding site. J Biol Chem 1997;272:23247–54.
36. Mukohara T, Engelman JA, Hanna NH, et al. Differential effects of gefitinib and cetuximab on non-small-cell lung cancers bearing epidermal growth factor receptor mutations. J Natl Cancer Inst 2005;97:1185–94.
37. Janmaat ML, Rodriguez JA, Gallegos-Ruiz M, Kruyt FA, Giaccone G. Enhanced cytotoxicity induced by gefitinib and specific inhibitors of the Ras or phosphatidyl inositol-3 kinase pathways in non-small cell lung cancer cells. Int J Cancer 2006;118:209–14.
38. Pao W, Miller VA, Politi KA, et al. Acquired resistance of lung adenocarcinomas to gefitinib or erlotinib is associated with a second mutation in the EGFR kinase domain. PLoS Med 2005;2:225–35.
39. Kobayashi S, Ji H, Yuza Y, et al. An alternative inhibitor overcomes resistance caused by a mutation of the epidermal growth factor receptor. Cancer Res 2005; 65:7096–101.
40. Olayioye MA, Neve RM, Lane HA, Hynes NE. The ErbB signaling network: receptor heterodimerization in development and cancer. EMBO J 2000;19:3159–67.
41. Okabayashi Y, Kido Y, Okutani T, Sugimoto Y, Sakaguchi K, Kasuga M. Tyrosines 1148 and 1173 of activated human epidermal growth factor receptors are binding sites of Shc in intact cells. J Biol Chem 1994;269: 18674–8.
42. Riemenschneider MJ, Bell DW, Haber DA, Louis DN. Pulmonary adenocarcinomas with mutant epidermal growth factor receptors. N Engl J Med 2005;352:1724–5.
43. Shigematsu H, Lin L, Takahashi T, et al. Clinical and biological features associated with epidermal growth factor receptor gene mutations in lung cancers. J Natl Cancer Inst 2005;97:339–46.
44. Calvo E, Baselga J. Ethnic differences in response to epidermal growth factor receptor tyrosine kinase inhibitors. J Clin Oncol 2006;24:2158–63.
45. Sugio K, Uramoto H, Ono K, et al. Mutations within the tyrosine kinase domain of EGFR gene specifically occur in lung adenocarcinoma patients with a low exposure of tobacco smoking. Br J Cancer 2006;94:896–903.
46. Riely GJ, Pao W, Pham D, et al. Clinical course of patients with non-small cell lung cancer and epidermal growth factor receptor exon 19 and exon 21 mutations treated with gefitinib or erlotinib. Clin Cancer Res 2006; 12:839–44.
47. Jackman DM, Yeap BY, Sequist LV, et al. Exon 19 deletion mutations of epidermal growth factor receptor are associated with prolonged survival in non-small cell lung cancer patients treated with gefitinib or erlotinib. Clin Cancer Res 2006;12:3908–14.

Distinctive Evaluation of Nonmucinous and Mucinous Subtypes of Bronchioloalveolar Carcinomas in *EGFR* and K-*ras* Gene-Mutation Analyses for Japanese Lung Adenocarcinomas

Confirmation of the Correlations With Histologic Subtypes and Gene Mutations

Yuji Sakuma, MD, PhD,[1] Shoichi Matsukuma, PhD,[1] Mitsuyo Yoshihara,[1] Yoshiyasu Nakamura,[1] Kazumasa Noda, MD, PhD,[2] Haruhiko Nakayama, MD, PhD,[2] Yoichi Kameda, MD, PhD,[3] Eiju Tsuchiya, MD, PhD,[1] and Yohei Miyagi, MD, PhD[1,4]

Key Words: Lung; Adenocarcinoma; Bronchioloalveolar; EGFR; K-ras; Mutation; Loop-hybrid mobility shift assay

DOI: 10.1309/WVXFGAFLAUX48DU6

Abstract

*Although adenocarcinomas of the lung are associated with epidermal growth factor receptor (*EGFR*) gene mutations and sensitivity to EGFR tyrosine kinase inhibitors, it remains unclear whether bronchioloalveolar carcinoma (BAC) components and/or subtypes affect these associations. We aimed to clarify correlations between* EGFR *gene mutations and BAC components and to establish the histologic features as reliable predictors for the mutations. We examined 141 non–small cell lung cancers (NSCLCs), including 118 adenocarcinomas, for mutations in exons 19 and 21 of the* EGFR *gene together with mutations in codon 12 of the K-*ras *gene using loop-hybrid mobility shift assays, a highly sensitive polymerase chain reaction–based method. Adenocarcinomas were subdivided into subtypes with a nonmucinous or mucinous BAC component and those without BAC components.*

In NSCLCs, EGFR *mutations were detected in 75 cases (53.2%) and were significantly associated with adenocarcinoma, female sex, and never smoking. Among adenocarcinomas, nonmucinous and mucinous BAC components were significantly associated with* EGFR *and K-*ras *gene mutations, respectively. Because* EGFR *mutations were detected even in most pure nonmucinous BACs, ie, lung adenocarcinoma in situ,* EGFR *mutation is considered a critical event in the pathogenesis of nonmucinous BAC tumors.*

In non–small cell lung cancers (NSCLCs), activating mutations in the tyrosine kinase domain of the epidermal growth factor receptor (*EGFR*) gene have been reported to be associated with sensitivity to EGFR tyrosine kinase inhibitors (TKIs), such as gefitinib and erlotinib. Furthermore, *EGFR* mutations are more frequently observed in patients with adenocarcinoma, people who have never smoked, women, and Asian patients.[1-10] These findings greatly mirror the increased response rates to EGFR TKIs in these groups of patients with NSCLCs.[11] In vitro experiments revealed that an NSCLC cell line with an *EGFR* mutation was 50-fold more sensitive to growth inhibition by gefitinib than cell lines with wild-type *EGFR*. In addition, autophosphorylation (activation) of EGFR was completely inhibited in the presence of a 100-fold smaller concentration of gefitinib than that required to inhibit wild-type EGFR.[2]

In the revised World Health Organization classification of 1999,[12] bronchioloalveolar carcinoma (BAC) is defined as "an adenocarcinoma with a pure lepidic growth pattern and no evidence of stromal, vascular or pleural invasion and subdivided into nonmucinous, mucinous or mixed type." Formerly, however, BAC cases were subclassified into mucinous, nonmucinous, and sclerotic subtypes, and a subset of the sclerotic type of BACs included clearly focally invasive adenocarcinomas with a lepidic growth pattern.[13,14] Because according to the 1999 World Health Organization classification most lung adenocarcinomas with a BAC component are now classified as adenocarcinoma, mixed subtype, the classification of BACs of the lung has remained controversial. The reported correlation between BAC histologic features and response to gefitinib is also controversial owing to the terminology. Miller et al[15] reported that a good response to gefitinib was more frequently

found in patients with "adenocarcinoma of the bronchioloalveolar subtype." Subsequently, several reports showed that adenocarcinomas with a BAC component were significantly correlated with *EGFR* mutations,[1,3,16-18] although other studies did not confirm the correlation.[6,8,9]

Mutations in K-*ras*, a known downstream signaling molecule in the EGFR signaling pathway, have been detected in a subset of lung adenocarcinomas. Interestingly, most mucinous subtypes of BAC have been reported to harbor K-*ras* mutations.[14,19] Although nonmucinous and mucinous subtypes of BACs are clinically, biologically, and histologically distinct from one another,[14] most[1-4,6-10,15-17] (except a few[5,18]) reports have not subdivided the BACs into nonmucinous and mucinous subtypes, and, therefore, relationships between BAC subtypes and *EGFR* and K-*ras* gene mutations have remained unclear.

Since we previously developed a rapid, easy, and sensitive method for detecting known point mutations and deletion mutations,[20] we examined NSCLC specimens from Japan for mutations in *EGFR* exons 19 and 21 and K-*ras* codon 12 and analyzed the relationships between the *EGFR* or K-*ras* gene mutational status and clinicopathologic features, especially histopathologic features, to clarify the roles of *EGFR* and K-*ras* mutations in the pathogenesis of NSCLCs, especially adenocarcinomas. In addition, we examined adenocarcinoma specimens for expression and phosphorylation status of EGFR and analyzed the association between *EGFR* gene mutations and the expression level or phosphorylation status of EGFR.

Materials and Methods

Cases and Tissue Specimens

Surgically resected specimens of 141 primary NSCLCs, consisting of 118 adenocarcinomas, 2 adenosquamous carcinomas, and 21 squamous cell carcinomas, were obtained from Kanagawa Cancer Center Hospital (Yokohama, Japan) during the period from January 2002 to August 2004. Institutional review board permission and informed consent were obtained for all cases.

BAC was defined as an adenocarcinoma with a pure lepidic growth pattern and no evidence of stromal, vascular, or plural invasion, ie, a peripheral lung adenocarcinoma in situ.[12] In nonmucinous subtypes, the neoplastic cells are cuboidal and usually show apical snouts and a hobnailed appearance. In mucinous subtypes, alveolar walls are lined by a cellular proliferation of columnar cells with abundant apical mucin and small basally oriented nuclei.[12] Small peripheral lung adenocarcinomas are subdivided as follows: (1) with a BAC component (replacing growth type), which are further subdivided into pure BAC and mixed BAC and invasive components, and (2) without BAC components (nonreplacing and destructive growth type).[21]

In this study, all pathology slides of the 118 adenocarcinomas were reviewed and reclassified as follows: (1) adenocarcinoma with a nonmucinous BAC component (n = 82), including pure nonmucinous BAC (n = 17) and invasive adenocarcinoma with a nonmucinous BAC component (n = 65); (2) adenocarcinoma without BAC components (n = 27); and (3) adenocarcinoma with a mucinous BAC component (n = 9), including pure mucinous BAC (n = 2) and invasive adenocarcinoma with a mucinous BAC component (n = 7). These diagnoses were independently made by 3 pathologists (Y.S., Y.K., and E.T.). Discrepancies in diagnoses were resolved by mutual agreement. The 141 patients with NSCLC included 69 men and 72 women with a median age of 65 years (range, 39-86 years). The 118 patients with adenocarcinoma included 51 men and 67 women with a median age of 64 years (range, 39-86 years). In total, 105 patients had stage I disease, 13 had stage II, 22 had stage III, and 1 had stage IV. There were 64 patients who had never smoked and 77 who had, including 35 current and 42 former smokers.

Immunohistochemical Studies for EGFR and Phospho-EGFR

Formalin-fixed, paraffin-embedded tissue sections of the 118 adenocarcinomas were prepared. The level of EGFR expression was determined by immunohistochemical analysis using an EGFR PharmDx kit (k1492; DAKO Japan, Kyoto, Japan), according to the manufacturer's recommendations. Each slide was scored as positive if more than 5% of tumor cells had membranous staining. The membranous staining intensity was evaluated using a 0 to 3+ scale, in which scores of 0 or 1+ were considered negative for EGFR overexpression and scores of 2+ or 3+ were positive. The presence or absence of phosphorylated EGFR (phospho-EGFR) expression was determined by immunohistochemical analysis using a mouse monoclonal antibody, pY1173EGFR (K1497; kindly provided by DAKO Japan), which specifically recognizes phosphorylated tyrosine at codon 1173 of EGFR, according to the manufacturer's protocol. Each slide was considered positive if more than 5% of tumor cells exhibited membranous staining but negative if the staining was only cytoplasmic.

DNA Preparations and Plasmid Clones

Formalin-fixed, paraffin-embedded tissue sections were used for DNA isolation from the tumor tissues. Briefly, a drop of pinpoint solution (Pinpoint Slide DNA Isolation System; Zymo Research, Orange, CA) was applied to the exact area of the tumor, of approximately 5 × 5 mm^2, which was identified in H&E-stained serial sections, and DNA was extracted according to the manufacturer's instructions. Cloning of polymerase chain reaction (PCR) products into plasmids was carried out

DOI: 10.1309/WWXFGAFLAUX48DU6

using the TOPO-TA ligation vector, pCR4TOPO (Invitrogen, Carlsbad, CA). The cloned plasmids were amplified with Phi29 polymerase (Amersham Bioscience, Piscataway, NJ) and used for sequencing of the inserted tumor DNA fragments (CEQ8000 Sequence Analysis System, Beckman Coulter, Fullerton, CA).

Loop-Hybrid Mobility Shift Assay

The loop-hybrid mobility shift assay (LH-MSA)[20] consisted of 2 parts: (1) hybridization of PCR products with loop-hybrid generator (LH-G) probes of synthetic oligonucleotides (75mer to 99mer) to generate loop hybrids and (2) detection of retarded-mobility bands of the loop hybrids in native polyacrylamide gel electrophoresis. The nucleotide sequences of the PCR primers and LH-G probes used to detect hot spot point mutations (E7R for *EGFR* exon 21 at L858; K7F for K-*ras* exon 2 at G12) and deletion mutations (19JWTF for *EGFR* exon 19) in the present study are described in ▮Table 1▮.

PCR was performed with Accuprime *Taq* polymerase together with primer-template hybridization enhancing reagent (Invitrogen). Generation of loop hybrids was carried out at the end of the PCR amplification cycles by adding a specific LH-G probe into the PCR reaction solution to a final concentration of 500 nmol/L. The mixture was then treated by the loop-hybrid formation steps consisting of denaturation at 94°C for 2 minutes, hybridization of the LH-G probe to the complementary strand at 55°C for 15 seconds, and extension of the 3' end of the LH-G probe in loop hybrids by *Taq* polymerase at 68°C for 4 minutes. The reaction products after the loop-hybrid formation steps were subjected to polyacrylamide gel electrophoresis for detection of mobility-shifted loop-hybrid bands by mutations. The gels were stained with SYBER Green I (Cambrex Bio Science, Rockland, ME), and the DNA bands were detected with the laser scanning imager (STORM 860, GE Healthcare Biosciences, Piscataway, NJ). The DNA bands with mutations detected by the LH-MSA were cloned into plasmids and sequenced.

Statistical Analyses

We looked for associations between *EGFR* or K-*ras* mutations and various patient characteristics, including age, sex, smoking history, stage of disease, pathologic subtype, EGFR overexpression, and phospho-EGFR expression. The χ^2 test or Fisher exact test was conducted to analyze the associations between mutations and each of the potentially influential factors. The Fisher exact test was performed if there were 5 or fewer observations in a group. The Mann-Whitney *U* test was used to assess the relationships between *EGFR* mutations and the expression level of EGFR. To identify which independent factors had a significant influence on the incidence of *EGFR* or K-*ras* mutations, logistic regression models were used. Probability values of less than .05 were defined as statistically significant.

Results

EGFR Mutations in NSCLCs

▮Table 2▮ summarizes a total of 88 *EGFR* mutations among 75 NSCLCs detected in this study. *EGFR* mutations were detected in 75 (53.2%) of 141 patients with NSCLC ▮Image 1▮. Among the 75 patients with *EGFR* mutations, 13 (17%) had multiple mutations. We found that 40 (53%) had in-frame deletion mutations in exon 19, 26 (35%) had a point mutation in exon 21, and 9 (12%) had deletion and point mutations in exons 19 and 21, respectively. Among the 40 patients with deletion mutations, of whom 4 had double mutations, all 44 mutations occurred around codons 747 to 749 in exon 19. Among the 26 patients with a point mutation in exon 21, 24 had an L858R mutation. In the 9 patients with both exon 19 deletion and exon 21 point mutations, all 9 of the 9 deletion mutations and most (8/9 [89%]) of the point mutations occurred around codons 747 to 749 and at codon 858, respectively.

▮Table 1▮
PCR Primers and LH-G Probes Used for Detection of Mutations in *EGFR* and K-*ras*

Gene	Mutation	Amplicon (bp)	PCR Primer	LH-G Probe† (Probe Name)
EGFR	In-frame deletion in exon 19	212	F: GGACTCTGGATCCCAGAAGGTG; R: CATTTAGGATGTGGAGATGAGC	GGACTCTGGA TCCCAGAAGG TGAGAAAGTT AAAATTCCCG TCGCTATCAA GGAATTAAGA GAAGCAACAT CTCCGAAAGC CAACAAGGAA ATCCTCGAT (19JWTF)
EGFR	Point mutation in exon 21 at L858	161	F: GGCATGAACTACTTGGAGGAC; R: CTTACTTTGCCTCCTTCTGCATG	CTTACTTTGC CTCCTTCTGC ATGGTATTCT TTCTCTTCCG CACCCAGCAG *******AGC CCAAAATCTG TGATCTTGAC ATGCTGCG (E7R)
K-*ras*	Point mutation in exon 2 at G12	165	F: AAGGCCTGCTGAAAATGACTG; R: GGTCCTGCACCAGTAATATGCA	AAGGCCTGCT GAAAATGACT GAATATAAAC TTGTGGTAGT TGGAGCTGG* ******GGCA AGAGTGCCTT GACGATACAG CT (K7F)

bp, base pairs; EGFR, epidermal growth factor receptor; F, forward; LH-G, loop-hybrid generator; PCR, polymerase chain reaction; R, reverse.
†Asterisks indicate deleted nucleotides; underlined type, nucleotides for the hot spots of mutations to be detected.

DOI 10.1309/WVXFGAFLAUX48DU6